P-58

LONG-TERM PREDICTION TEST PROCEDURE FOR MOST ICs, BASED ON LINEAR RESPONSE THEORY

Final Report

April 1, 1991

by

V. Litovchenko and I. Ivakhnenko

Contract Number NAG-5-864

Vitreous State Laboratory
The Catholic University of America
Washington, D.C. 20064

ABSTRACT

Experimentally, thermal annealing is known to be a factor which enables a number of different integrated circuits (ICs) to recover their operating characteristics after suffering radiation damage in the space radiation environment, and thus to decrease and limit long-term cumulative total-dose effects. This annealing is also known to be accelerated at elevated temperatures both during and after irradiation.

We have applied linear response theory (LRT) and have constructed a linear response function (LRF) to predict the radiation/annealing response of sensitive parameters of ICs for long-term (several months or years) exposure to the space radiation environment.

In order to develop a short-term (several hours or days) test procedure for predicting long-term annealing, a number of LRF constants in this theoretical model must be determined. Several methods to calculate the LRF constants from the experimental data have been used. Equations for the shift in the threshold potential of MOS ICs have been derived for both pure annealing and simultaneous irradiation and annealing. Estimations of the equilibrium point of the shift in the threshold potential have been made.

Since we need to conduct a short-term test to make predictions of the radiation response for the very long-term region of the IC's operation, a compression in time was proposed. Compressing the annealing process from several years in orbit to just a few hours or days in the laboratory is achieved by subjecting the IC to elevated temperatures or by increasing the typical spaceflight dose rate by several orders of magnitude for simultaneous radiation/annealing only.

The development of tests at elevated temperatures was based on linear response theory and theoretical models in order to use data extrapolation from the elevated temperatures to near-room temperature. To use LRT, we need to check the linearity of the response with respect to impulse dose for pure annealing and with respect to dose rate for simultaneous irradiation and annealing. This approach became a part of the test development.

The test procedure to make predictions of the radiation response was developed; the calculation of the shift in the threshold potential due to the charge distribution in the oxide was written; electron tunneling processes from the bulk Si to the oxide region in an MOS IC were estimated; in order to connect the experimental annealing data to the theoretical model, constants of the model of the basic annealing process were established; experimental data obtained at elevated temperatures were analyzed; time compression and reliability of predictions for the long-term region were shown; a method to compress test time and to make predictions of response for the non-linear region was proposed; non-linearity of the LRF with respect to log(t) was calculated theoretically from a model.

INTRODUCTION

This work deals with the development of a test to predict the radiation/annnealing response in sensitive parameters of ICs in long-term operation in a radiation environment.

Semiconductor ICs installed in electronics, computers and other systems of spacecraft, nuclear power installations (submarines in particular) and particle accelerators suffer total-dose , slow-rate radiation damage, which usually appears as a change in operating characteristics. Although total-dose radiation damage is cumulative, in the slow-rate radiation environment, such as in space, nuclear power installations and particle accelerators, annealing has been observed to occur in many IC technologies. After some time in the radiation environment, it is expected that a situation will be reached in which the annealing rate will match the damage introduction rate and will result in stability of the shift in the sensitive parameter, for example, in the threshold potential for MOS ICs. For the electronics to be operational after this time in the radiation environment, it is necessary to determine whether or not the parameters of the device are still within specifications.

Flight projects and equipment designers are consequently asking how much annealing can be expected to extend the operating time of ICs and other devices for long-term use in radiation environments in space and on Earth. An easy way to answer these questions would be to allow the damaged devices to anneal for two or three years at room temperature and observe the results of annealing. Such tests, however, would be time-consuming and impractical.

Yet, the problem is still not solved, although constant attempts have been made to choose the most radiation-resistant devices and to choose such a technology in a short-time test. Hence, a number of tests have been proposed[18-21].

1. Such a test[18] has been performed: a detailed comparison of 1/f noise with the radiation-induced threshold voltage shifts due to oxide-trapped charge and interface states for enhancement-mode, 3-nm gate, n-channel MOS transistors. It was shown that the pre-radiation 1/f noise levels of these devices correlated strongly with the post-radiation threshold shift component and was related to the oxide traps, ΔV_{ot}, but not with the post-radiation shift component related to the interface states, ΔV_{it}. These results are supposed to show that 1/f noise measurements may prove useful in characterizing and predicting the response of MOS devices.

This test cannot give correlations of the pre-radiation 1/f nose with the post-radiation ΔV_{it} which is one of the components of the radiation-induced shift in the threshold potential. The problem of long-term prediction of the radiation-induced shift in the threshold is not approached.

2. In the second work[19], a simple model was suggested to interpret and to extrapolate the experimental data by fitting the data to the model.

This investigation suggests a test procedure, using a simple linear dependence on log(t) of annealing, which does not work for the long-term period. Also, this test procedure consumes as much time as a simple long-term experimental test, because annealing in this test was not accelerated.

3. The third and fourth tests[20-21] that were proposed used a compression of time by using elevated temperatures. These completely empirical tests could only classify the MOS devices into particular groups. Their main goal is to predict the grade of radiation hardness of a device, but not the value of the radiation-induced shift in the threshold potential or the shift in other sensitive parameters.

A number of tests suggest simply applying an increased dose rate, i.e., to irradiate a device to the total required dose in a short time, but a difference between prediction and response has been observed.

We are going to make predictions, for example, of the shift in the threshold potential, by applying the LRT. We are determining the region of linearity of the response relative to an impulse dose for pure annealing and the linearity of the radiation response relative to the dose rate for simultaneous radiation and annealing. For the linear region, the LRT will be used as the principal tool and the damaged devices will be subjected to elevated temperatures to accelerate the annealing. This method was proposed to shorten the time period of the tests and to use the results of these tests to predict the anticipated long-term annealing.

These short-term (several hours or days) test procedures for making predictions for long-term (several months or years) radiation/annealing response of ICs in a radiation environment were developed for linear and non-linear response relative to dose rate. For the non-linear region, the method of increasing the dose rate to shorten the test time was proposed. Also, the quasi-linear approach to calculate a prediction of response was introduced for non-linear cases.

Calculations were made to predict when the simultaneous irradiation/annealing can be expected to reach an equilibrium. The maximum value of the shift in the threshold potential, V(t), (equilibrium value) was estimated. Experimental data were treated according to the LRT and results produced the LRF shape and time compression rate for the long-term region. The shift in the threshold potential was introduced by calculating the electric field distribution in relation to the charge distribution in the bulk oxide. The deviation of the LRF from linear dependence on log(t) was derived theoretically from the model. We also observed cases of high-dose-rate radiation damage and a high-dose impulse radiation environment, where linearity of radiation response relative to dose and dose rate does not exist. To make predictions of the malfunctioning of ICs in this case, a time compression of the test by increasing the dose rate was proposed.

THEORETICAL MODEL

LINEAR RESPONSE MODEL

The Concept of Impulse Dose and Impulse Response

According to linear response theory (LRT), radiation response, i.e., shift in the sensitive parameter, of any device subjected to a radiation environment is linearly proportional to an impulse dose, if this impulse dose is small and the instant of measurement of the response is far removed in time from the instant of the impulse dose, as in Fig.1:

$$\Delta P(t) = R(t)\Delta D, \tag{1}$$

where the linear response function (LRF), R(t), depends on a time lapse:

$\Delta P(t) = R(t-t')D(t')$

and the LRF, R(t), can be determined to be:

$R(t) = \Delta P/\Delta D.$

To determine the region of linearity, one has to plot ΔP measured at a fixed instant, t, as a function of ΔD, as shown in Fig.2.

In this work, we have used linear response theory to solve both cases of pure annealing (from impulse and non-impulse doses) and simultaneous irradiation and annealing. Since we are applying LRT, i.e., a linear approach, to experimental data during the test, the concept of impulse dose is crucial for our work. The calculations of threshold potential as the main sensitive parameter for MOS devices for both pure annealing and simultaneous irradiation and annealing are essential. Calculations will determine whether the concept of impulse dose can give us:

1. The practical time duration of the impulse dose and

2. The limit of radiation dose magnitude.

Some simple transformation would be helpful. The shift in the main MOS IC parameter, the threshold potential can be determined from linear response theory as shown below:

$$\Delta V(t) = \dot{D}\int_0^{t_r} R(t-j)\,dj = -\dot{D}\int_{t-t_r}^{t} R(t')dt',$$

where the dose rate, $\dot{D}$ = const. and R(t) is the linear response function. Such a transformation yields the threshold shift calculation,

$$\Delta V(t) = \dot{D}[F(t) - F(t-t_r)], \text{ where } F(t) = \int_0^t R(t')dt.$$

Expanding the equation for the response shift in a Taylor power series for small irradiation time, t_r and using the equation for the linear response function,

$$R(t) = -C + A \ln(t/t_0),$$

we then obtain:

$$\Delta V(t)/D(t_r) = -C + A \ln(t_r/t_0) + K + T,$$

where $T = (A/2)t_r/t$ and $K = A(t_0/t_r)(t - t_r)/t_0$.

We can then calculate the conditions for choosing the observation time, t, and the irradiation time, t_r, such that the dose response is linear. Knowing that $t_r < t$, $T/K = t^2_r/2t^2$. Let us set this expression equal to 1/100. This means that, in the expression involving the observation time, t, and the irradiation time, t_r, the deviation of response from linearity in log(t), T, has the value of 1/100 of the second term of the expansion, therefore t_r/t should be less than 1/7, i.e., on the order of 1/10.

The concept of impulse dose and the condition of linearity are sources of the method for determining the linear response function from experimental data for the linear case. The method to determine the limit of radiation dose magnitude from the experimental data is shown in Fig.2.

Using this basic concept, we can obtain experimental data to investigated the critical region of time dependence of the radiation damage response during which equilibrium between the radiation damage rate and annealing rate occurs. , In this area, the linear response function, as will be shown, changes its character, and to make predictions for long-term operation (from several months to a few years), we must determine the Linear Response Function for long-term annealing, using experimental data.

The linear response theory for the case of pure annealing, as well as simultaneous irradiation and annealing, will be directly applicable to spacecraft flown in the space radiation environment, where both radiation damage and annealing take place at the same time.

In the case of non-linear response, an approach to solve the problem will be shown below.

1. Pure annealing in MOS devices

Much work has been done in the area of radiation or radiation sensitivity of MOS ICs. Some work has been done on pure annealing and very little, if any, has been done on the simultaneous radiation and annealing response.

Linear response theory presumes that the annealing of a sensitive parameter is linearly proportional to the imparted impulse radiation dose and depends on the time lapse between the observation time and the time of the imparted impulse dose, as shown in Fig.1.

There are several sensitive parameters of a MOS integrated circuit which can be used to measure damage and annealing, such as the shift in the threshold potential, $\Delta V(t)$, of individual transistors, leakage currents, propagation delay, rise and fall times, etc. Since the device parameter, the shift in the threshold potential, expressed as $\Delta v(t)$, is most often used as the sensitive parameter, we choose to use this parameter in our measurements of annealing. Eq.(1) thus becomes

$$\Delta V = R(t-t')\Delta D(t'). \tag{2}$$

In the case of many impulse doses, the total annealing response is the result of the sum of the partial response. In the case of continuous irradiation, this becomes an integral

$$\Delta V(t) = \int_0^t R(t-t')dD(t'). \tag{3}$$

1.1 Determination of Response Function

In the case of pure annealing, we shall use Eq.(2) to determine R(t). For this purpose, we set $t' = 0$. Then

$$\Delta V(t) = R(t)\Delta D(0),$$

and the response function becomes

$$R(t) = \Delta V(t)/\Delta D(0),$$

which turns out to be the remainder of the gate threshold voltage shift per unit dose at time, t, far removed from the impulse dose, i.e., $t' << t$.

Pure annealing has been observed by several investigators to be nearly linear with respect to the logarithm of annealing time. Danchenko at al.[1] observed a linear or

near-linear dependence on log(t) of annealing in a pMOS device. A similar log(t) dependence for other technologies was observed by Simons and Hughes[2,3] and Simons[4]. The only deviations from this linear dependence are observed at very short and very long annealing times.

These experimental data show that R(t) plotted vs. ln(t) follows a near-straight line. Under this assumption, for pure annealing, R(t) takes the form:

$$R(t) = -C + A \ln(t)$$

where the coefficients A and C are regarded as independent of impulse dose and should be determined experimentally.

To render the argument of R(t) dimensionless, it is necessary to introduce another parameter, the characteristic time, t_0, which is related to the annealing rate. The response function thus becomes

$$R(t) = -C + A \ln(t/t_0). \tag{6}$$

To find the significance of the constants A, C and t_0, we have plotted R(t) (as given by Eq.(6)) vs. ln(t), as shown in Fig.3. To separate the constants from ln(t), we have transformed this equation as follows:

$$R(t) = [-C - A \ln(t_0)] + A \ln(t).$$

As can be seen from Fig.3, the region $t_0 << t < t_c$ represents a straight line in R(t). If we extrapolate this straight line to ln(t) = 0, we see that it intercepts the ordinate at $[-C - A \ln(t_0)]$. We can determine A immediately, since it is the slope of a straight line. C and t_0, however, cannot be separately determined, because they are factors of the intercept, $[-C - A \ln(t_0)]$. A few methods exist to find C and t_0. To find C, one can measure the response at $t << t_0$ and obtain

$$R(t) = \Delta V(t)/\Delta D = C - a_1(t/t_0) + a_2(t/t_0)^2 + \ldots$$

To make the function valid in the region of small t, we can change the argument of Eq.(6) as follows:

$$R(t) = -C + A \ln(1 + t/t_0). \tag{7}$$

We can plot this equation for small t . We can see that, as t approaches zero, ln(t) approaches minus infinity and R(t) approaches (-C).

For large t, we can estimate at what time annealing will be nearly complete. When we extrapolate the linear region of the curve in Fig.3 to $R(t) = \Delta V/\Delta D = 0$, we obtain a rough estimate of the critical time, t_c, given by:

$$-C + A \ln(t_c/t_0) = 0, \text{ or } t_c = t_0 \exp(C/A). \tag{8}$$

This estimate of t_c is valid for pure annealing, as well as for simultaneous irradiation and annealing, as we will see below.

We also need to determine at what time the straight line of R(t) (Fig.2) intercepts the straight line of (-C). We can immediately determine this time, $t = t_0$, and $R = R(t_0) - (-C) = A \ln(2)$.

1.2 Generalized Convolution Integral.

Response to continuous irradiation can be described as a sum of responses to a number of impulse doses. Such a response can be calculated as an integral:

$$\Delta P(t) = \int_0^t R(t-t')\dot{D}dt'.$$

If the radiation ceases at time, $t_r < t$, then

$$\Delta P(t) = \int_0^{t_r} R(t-t')\dot{D}dt'.$$

If $tr << t$, then $t' << t$ and $R(t-t') = R(t)$. Then:

$$\Delta P(t) = R(t)\int_0^{t_r} \dot{D}dt;, \text{ or}$$

$\Delta P(t) = R(t)D(t_r)$. In other words, for $t >> t_r$, the total dose, $D(t_r)$, may be regarded as an impulse dose.

Using the gate threshold potential as a sensitive parameter, and assuming that the total imparted dose is not an impulse dose, but is extended in time, we can derive the same equation, integrating Eq.(2) over the period of time in which irradiation occurs. We thereby obtain the same convolution integral in the form:

$$\Delta V(t) = \int_0^{t_r} R(t-t')\dot{D}dt',$$

where t_r is the time at which irradiation ceases.

In the case of pure annealing, t_r is always less than t. If $t_r << t$, then Eq.(9) takes the form:

$$\Delta V(t) = R(t)D(t_r), \qquad (10)$$

which is similar to Eq.(2) and gives us the response function as the shift in threshold potential per unit total dose.

2. Simultaneous Irradiation and Annealing

As has been shown, calculations developed for pure annealing can also be applied to simultaneous irradiation/annealing with some modification if the linearity of radiation response relative to dose rate (or accumulated dose) exists.

21. The linearity of Response Relative to Dose Rate

During long-term spaceflight, the irradiation/annealing response of a device in the space radiation environment could become non-linear. To make predictions correctly, we need to determine the region of linear response with respect to dose rate for long times, as in Fig.4.

We can find the slope in Fig.4: $\Delta P = D \times \text{Slope}$; t is large and

$$\text{Slope} = \int_0^t R(t')dt'.$$

This relation and determination of linearity of the response with respect to dose rate will be used in the test procedure.

2.2 Calculations of Response

Derbenwick and Sander[5] were the first to suggest the applicability of linear response theory to annealing through the use of a convolution integral. Winokur et al.[6,8] have also made extensive use of a convolution integral in their analysis of experimental data. The authors applied the convolution theory to calculate the radiation-induced voltage shifts for a uniform dose rate:

$$-\Delta V(t) = Bt\{-A[x \ln(x/x-1) + \ln(x-1)] + (A + C)\},$$

where $x = t/t_e$, B is equal to a constant dose rate and A is the annealing rate. In this equation, they explained the time, t, as the time at which the measurement is taken and the time, t_e, as the time of termination of the radiation exposure at a constant dose rate.

Applying a convolution integral, we set the time of cessation of irradiation, t_r, equal to the time of observation, t, in Eq.(9), which yields:

$$\Delta V(t) = \int_0^t R(t-t')\dot{D}dt'. \tag{11}$$

In order to find an expression for the threshold potential shift, $\Delta V(t)$, we substitute Eq.(7) into Eq.(11). Integrating Eq.(11), we obtain:

$$\Delta V(t) = [A(1 + t_0/t) \ln(1 + t/t_0) - (A + C)\dot{D}t, \tag{12}$$

where $\dot{D}$ is assumed to be constant with respect to time.

For $t >> t_0$, Eq.(12) becomes:

$$\Delta V(t) = [A \ln(t/t_0) - (A + C)]D(t), \tag{13}$$

where the total dose, D(t), is equal to $\dot{D}t$, or:

$$[\Delta V] = \dot{D}t[A + C - A \ln(t)]. \tag{13'}$$

$\Delta V(t)$ and $\Delta V(t)/\dot{D}t$ expressed in Eqs.(12), (13) and (13;) are plotted vs. ln(t) in Fig.5 and Fig.6 for arbitrary values of the constants.

It is anticipated that in space (and in similar radiation environments), as the damage accumulates, a time will be reached when the damage introduction rate will be balanced by the annealing rate and the threshold potential will reach stability. This region of balance is shown in Fig.5 for large t.

A useful approach to treat the experimental data of very long-term simultaneous irradiation and annealing is to plot $\Delta V(t)$ per unit dose, instead of $\Delta V(t)$. In Fig.6, we plot $\Delta V(t)/D(t)$ vs. ln(t). Indeed, we see that, for large t, we have a straight line, in accordance with Eq.(13), plotted as:

$$\Delta V(t)/D(T) = A \ln(t/t_0) - (A + C). \tag{14}$$

We have the experimental evidence to prove such a conclusion. Curves of simultaneous irradiation and annealing from experimental work[26] with supplemented "straight line" curves of $\Delta V/D$ calculated from these experimental data are shown in Figs. 24 and 25.

In time, however, we should see some deviation from this straight line, as in the case of pure annealing. This region of deviation, t_d, is important for the treatment of experimental data, because this is the region to which the saturation of the damage or the balance between the damage introduction rate and annealing rate is very close. In the laboratory, we can investigate this region experimentally, since, at elevated temperatures, the deviation can be observed in a short time. We consequently have to investigate this region in detail.

The straight line of Fig.6, plotted vs. ln(t), intercepts the $\Delta V(t)/D(t) = 0$ axis either at $\ln(t/t_0) = C/A + 1$, or explicitly at the critical time

$$t_c = t_0 \exp(C/A + 1). \tag{15}$$

This is a good approximation of the region in which the deviation occurs. In reality, however, we may expect the deviation to take place before this approximation, or before the minimum of Eq.(12). This minimum is given by

$$d[\Delta V(t)]/dt = A \ln(t/t_0) - C = 0. \tag{16}$$

This yields as a solution, $t_b = t_0 \exp(C/A)$, which is identical to Eq.(8). This implies that t_b is both the critical time for pure annealing and the theoretical equilibrium time, t_b, when balance between the damage introduction rate and the annealing rate occurs. Substituting t_b into Eq.(13), we obtain $\Delta V(t_b) = \Delta V_m$, which is the maximum value of $\Delta V(t)$:

$$\Delta V = -A\dot{D}t_b = -A\dot{D}t_0 \exp(C/A). \tag{17}$$

We can also determine another characteristic time, the time for half recovery, $t_{1/2}$, from Eq.(6) for pure annealing:

$$t_{1/2} = t_0 \exp(C/2A), \tag{18}$$

which is convenient for the treatment of experimental data.

PREDICTION OF LONG-TERM IRRADIATION/ANNEALING RESPONSE

The long-term irradiation/annealing response (from several months to a few years) is related to the region which includes t_d or close to it. For this long-term region,the case of non-linearity of radiation response relative to dose rate can be predicted by shortening the time duration of the test with increasing dose rate, D.

We can increase the dose rate by three orders of magnitude and shorten the time duration by the same factor and have close to the same value of the response. From the family of response curves shown in Fig.7, we can extrapolate the value of the time of deviation for flight conditions and time compression rate for a flight dose rate, as in Fig.8.

In Figs.8 and 10, the method to make predictions of the radiation response from data extrapolation is shown. Using the time deviation determined from the extrapolation described in Fig.7, we can calculate the time compression rate relative to the increased dose rate.

HIGH-DOSE IRRADIATION CASE

There is a wealth of experimental works which support the linear response theory and indicate that the differential response is linear with impulse dose. However, any physical system can exhibit a linear response only through a limited range of input. Obviously, the shock to a system by a strong input is non-linear, especially when the system is destroyed.

Although it is obvious that linear response theory cannot be applied for large dose rates or doses, there have so far been no attempts to determine the limits of dose or dose rate within which the system still exhibits a linear (with dose) response.

A number of projects strongly need the theoretical foundation and experimental research which we propose here. Such a theoretical investigation can be used to find the region of applicability of the linear response theory (LRT) as well as to develop a generalized response theory (GRT). It seems promising that such a generalized response theory can become the necessary tool, not only for the treatment of large total doses and dose rates, but also for the case of low-dose irradiation in the region of balance, when the damage introduction rate is equal or nearly equal to the rate of annealing.

As is known from the previous part, Eq.(1) states the experimental fact that the differential response is proportional to an impulse dose. By increasing the impulse dose, we step to the case in which the response becomes proportional to some function of dose, D, rather than the dose itself:

$$\text{(Change in sensitive parameter)} = R(t\text{-}t')\,F(D(t')). \tag{H1}$$

In the case of MOS ICs, this looks like

$$\Delta V(t.,D) = R(t\text{-}t;)\,F(D(t')). \tag{H2}$$

For a single impulse dose, it is convenient to set $t' = 0$. Then Eq.(H2) becomes

$$\Delta V(t, D) = R(t)\,F(D). \tag{H3}$$

For a fixed dose, D, one can determine R(t) as

$$R(t) = \Delta V(t, D)/F(D). \tag{H4}$$

To determine the exact value of F(D), one must impose the condition that, at the small-dose limit, F/D approaches unity.

To determine the response for continuous irradiation, one must integrate Eq.(H2) over the irradiation time, tr,

$$\Delta V(t, D) = \int_0^{t_r} R(t\text{-}t')\,dF(D(t')), \tag{H5}$$

or

$$\Delta V(t, D) = \int_0^{t_r} R(t\text{-}t')\,F'(D)\,dD(t') = R(t)\,F(D(t_r)). \tag{H6}$$

For the case in which the observation time, t, is far removed from the end of irradiation, i.e., $t >> t_r$, $R(t\text{-}t') = R(t)$, and Eq.(H5) yields

$$\Delta V(t, D) = R(t)\int_0^{t_r} dF(D) = R(t)\,F(D(t_r)). \tag{H7}$$

Since the response, $\Delta V(t, D)$, is a product of two functions, each dependent on its own variables, both the functions R(t) and F(D) can be determined. Then the response is totally described by Eq.(H5).

THEORETICAL APPROACH TO THE MODEL

The theoretical models[13-16] of basic internal processes in ICs, especially MOS ICs, developed by various authors, were used to work out the common theoretical base of the damage/annealing test. We will use these models of basic processes contributing to the radiation response and annealing, and, consequently, to the various constants of the LRF and their time-temperature dependence, especially the intensity of annealing, A, to develop a link between the macroscopic (and phenomenological) LRT approach, and microscopic processes. The schematic review of such basic processes and, in particular, the annealing process of charge buildup is shown in Figs.11 and 12.

From experimental data, we also know that, in the long-term region, the shift in the threshold potential changes its behavior. Thus, we see some deviation from a straight line,i.e., the form of the previously-developed LRF vs. ln(t). We can use the annealing data of this region of deviation (i.e., the long-term region) to determine the LRF constants for this region to treat annealing test data at elevated temperatures, as was previously shown, and to convert these data to normal temperatures for making predictions of the long-term radiation/annealing response for long-term operation. In order to make such an approach reliable, calculations of temperature dependence of LRF constants in the long-term region through theoretical models of the processes in the bulk oxide are essential.

From the experimental and theoretical works[22,23], which are consistent with each other, it is known that the basic model of the positive hole trap refers to the trap structure as a neutral center in the oxide with a ground state (singlet) below the Si valence band edge and an excited triplet state above the Si conduction band edge, as is shown in Fig.13.

Annealing in these models is considered to be tunneling of electrons directly from the bulk Si to the charged hole trap in the oxide. The formulation of this problem corresponds to the case in which a current of electrons is incident on the potential barrier.

The problem is related to the problem of determination of the probability of tunneling of electrons into the bulk oxide. Assuming electrons are being transported through the Si-SiO_2 interface from the Si valence band to the ground state of the hole trap center, as the best-known model of McLean indicates, we can write

$$p_{tun} = a \exp(-bx),$$

where a is the escape frequency and b is connected to the tunneling barrier. The probability of this tunneling depends exponentially on the tunneling distance from the hole trap to the interface.

According to the models[13, 24], the rate of charge loss from the oxide, or the rate of neutralizing of trapped holes inside the oxide is given by the differential equation:

$$dp(x, t)/dt = -a \exp(-bx)\, p(x, t),$$

where p(x, t) is the density of charged trapped holes in the oxide.

This equation yields

$$p(x, t) = p_0(x) \exp(-a \exp(-bx)t),$$

where $p_0(x)$ is the initial distribution of trapped holes inside the oxide as a function of x, which is a coordinate perpendicular to the oxide-silicon interface. These models have used the concept of the tunneling front, i.e., the x-position, x_m, of a surface at which the maximum rate of tunneling is occurring. So, we can obtain this position of x_m by differentiating the previous equation of p(x, t)/dt with respect to x and setting the result equal to zero:

$$x_m = (1/b) \ln(at). \qquad (D0)$$

This equation was used in direct calculation of the shift in the threshold potential in Eqs.(D22) and (D23).

Direct calculation of shift in threshold potential

As is already known, ionizing radiation in MOS devices generates trapped positive charge in the oxide layer and negative interface states which cause a shift in many parameters for the MOS device, such as threshold potential, leakage current, noise, capacitance, etc. To analyze these shifts, we developed a direct calculation, applying Maxwell's electromagnetic theory.

Though our primary goal is to deal with ionizing radiation, the method is also applicable to deal with any net charge inside a system, regardless of how the charge was created. For example, in the case of the theory of the new generation of electrical charge memories, we can apply this method.

Calculating the shift in the threshold potential, we assume that the processes are slow enough to apply the quasi-static approach.

Maxwell's equation relates displacement field, D, and density of charge, p,

$$\nabla \mathbf{D} = p.$$

We assume that the x-axis is perpendicular to the oxide/semiconductor interface, $x = l_{ox}$ at the interface, and $x = 0$ at the metal/oxide interface. We also assume that the

charge density, p(x, t), is independent of the two other spatial variables. In this case, the displacement, D, also depends only on the distance, x, (and time) and is perpendicular to the interface, i.e., D = D(x, t) and

$$dE(x, t)/dx = (1/\varepsilon_0\varepsilon)\, p(x, t), \tag{D1}$$

where $E = ((1/\varepsilon_0\varepsilon)D$ and ε_0 and ε are the dielectric constants. Integrating Eq.(D1), we obtain

$$E(x) - E(0) = (1/\varepsilon_0\varepsilon)\int_0^x p(x, t)\, dx, \tag{D2}$$

where the integral is the charge inside the oxide layer between x = 0 and the current coordinate x, per square unit of the interface, i.e., Q(x, t)/S. In this case, the potential difference can be calculated from:

$$E = -\nabla V. \tag{D3}$$

However, a variable electric field creates a variable magnetic field, H, in accordance with Maxwell's second equation:

$$\nabla \times H = j + \varepsilon_0\varepsilon\, \partial E/\partial t,$$

where j is electric current.

In electromagnetic theory, instead of Eq.(D3), one must use the following equation:

$$E = -\nabla V + \partial A/\partial t, \tag{D4}$$

where the vector potential, A, defines the magnetic field by the equation:

$$H = -[\nabla \times A],$$

satisfying the third Maxwell equation: $[\nabla \times H] = 0$ or $[\nabla \times \nabla \times A] = 0$. Eq.(D4) satisfies the fourth Maxwell equation:

$$[\nabla \times E] = -\partial H/\partial t, \text{ since } \nabla \times \nabla V = 0.$$

Taking into consideration the fact that the annealing process is slow from the electromagnetic point of view, we can neglect the magnetic field using the quasi-static approach. Eq.(D4) then takes the form:

$$E(x, t) = -dV(x, t)/dx. \tag{D5}$$

The net oxide positive charge, Q, is given by:

$$Q = S\int_0^{l_{ox}} p(x)\,dx, \tag{D6}$$

where l_{ox} is bulk oxide thickness, p(x) is charge density and S is bulk crossection. The shift in threshold potential ΔV, due to the net oxide positive charge, is thus given by:

$$\Delta V = -\int_0^{l_{ox}} E(x)\,dx, \text{ or}$$

$$\Delta V = -(1/\varepsilon_0\varepsilon)\int_0^{l_{ox}} dx \int_0^{x} p(x', t)\,dx'. \tag{D7}$$

The equation we have just derived is quite general. It relates only to charge distribution and may be applied for any method of charge generation and compensation, for pure annealing, for simultaneous irradiation and annealing and any kind of charge injection. For example, this equation enables us to investigate the silicon-nitride-oxide-silicon (SNOS) memory device. Unlike an MOS device, the main goal is to trap the positive or negative charge injected through the oxide into the nitride by a positive or negative voltage pulse applied to the gate of the SNOS transistor. The negative or positive potential shift is associated with a logic "0" or "1" state, respectively. In this case, we could be interested in as slow annealing as possible.

In deriving Eq.(D7), we neglected the magnetic field and its influence on the electric field, i.e., the electromagnetic waves. In order to justify this approximation, we need to estimate the order of magnitude of the wavelength of the main harmonic, representing the vector potential as a Fourier integral over a range of frequencies:

$$A(t) = (1/2\pi)\int A(\omega)\exp(i\omega t)\,d\omega,$$

where $A(\omega)$ has a maximum at $\omega_0 = 1/t_{ch}$ and decreases to zero rapidly for $\omega < \omega_0$ and $\omega > \omega_0$ and t_{ch} is the characteristic time, which determines the time scale for significant changes in A(t).

If the time scale, as in the case of annealing processes, is on the order of 10^{-4} sec., the characteristic electromagnetic wavelength for these processes can be estimated as:

$$\Lambda \sim c/\omega \sim 3 \times 10^6 \text{ cm},$$

where c is the velocity of light.

Obviously this electromagnetic wavelength is extremely large, and the corresponding magnetic field can thus be neglected.

Considerable work has been done to analyze the mechanisms contributing to the degradation of net charge. Physical models have been derived based on these mechanisms. The advantage of Eq.(D7) is its possibility to be applied to any particular mechanism of charge generation and degradation, or even to a combination of several mechanisms.

Damage Introduction Rate and Annealing Rate for McLean Model

First of all, we make use of Eq.(D7), derived above, calculating the response, $\Delta V(t)$, the relaxation of buildup of the net charge, not only to describe pure annealing, but also simultaneous irradiation and annealing.

We apply Eq.(D7) to relate the damage introduction rate, C, to the radiation-induced net charge, Q.

Suppose the impulse dose duration is much less than the characteristic time, $\Delta t << t_0$. This means that annealing has not started yet and we can obtain

$$\Delta V(\Delta t) = -[C - A \ln(1 + \Delta t/t_0)] \dot{D}\Delta t = -C\dot{D}\Delta t = -C\Delta D. \qquad (D8)$$

For a very short impulse dose (10^{-6} sec), we can assume uniformity of charge density inside the bulk oxide because of the incident character of primary ionization. We then obtain

$$\Delta V(\Delta t) = -C\Delta D = -Ql_{ox}/2\varepsilon\varepsilon_0 S, \qquad (D9)$$

where the net charge at time, t, is $Q = pl_{ox}S$.

For large impulse doses, 10^5 - 10^6 rad, a saturation effect may occur. Then, the dependence of the shift in the threshold potential ΔV, on total dose becomes non-linear:

$$\Delta V(\Delta t) = F(D).$$

On the other hand, the total charge, Q, is linearly proportional, with a coefficient, k, to the effective crossection, σ, the total number of atoms, $N = nl_{ox}S$, where n is atomic density, and the total dose, ΔD:

$$Q = k\sigma n l_{ox} S\Delta D. \qquad (D10)$$

By substituting Eq.(D10) into Eq.(D9), we obtain

$$C = k l_{ox}^2 n\sigma/\varepsilon_0\varepsilon. \qquad (D11)$$

The coefficient of proportionality, k, can be determined from independent measurements and can be calculated theoretically as well.

In Eq.(D8), we assumed a linear response, but linearity of response with dose should be confirmed and the boundary between the linear and non-linear approach should be determined, as we have shown in Fig.2.

The general equation (D7) can be used for any particular model of net charge buildup and relaxation, i.e., annealing.

McLean[13] suggested uniform charge distribution through a thin, 10 - 20 nm oxide layer near the Si-SiO_2 interface, with a sharp front of decreasing charge density moving from this interface through the bulk oxide to the metal. This model uses the advantage of the principle of a tunneling front, x_m, the location in the oxide at which the maximum rate of tunneling occurs.

The distance, x', from the Si-Sio_2 interface to the density front is proportional to ln(t).

The charge distribution can be presented as a step function (see Fig.14):

$$p(x, t) = \begin{cases} p_0, x' > x_m(t) \\ 0, x' < x_m(t), \end{cases} \qquad \text{(D12)}$$

where, according to Eq.(D0), $x_m = (1/b)\ln(at)$ or $x_m = x_0 \ln(t/t_0)$, p_0 is the charge distribution at $t = 0$ and x_0 is the width of the front.

The general equation (D7) can be used for any model and should be used for the previously cited McLean model, where the distance between the interface and the moving front is proportional to ln(t). It is also noted that the model can be applied for distances not less than 1.5 nm from the interface.

Since ln(t) cannot be used for $t = 0$, we substitute it with $\ln(1 + t/t_0)$. With this generalization, we can start from zero distance, $x = 0$ (or $x' = l_{ox}$), and $t = 0$. We thus assume that the front distance, $x_m(t)$ is given by:

$$x_m(t) = l_{ox} - x_0 \ln(1 + t/t_0), \qquad \text{(D13)}$$

the front velocity is:

$$v = x_0/(t + t_0), \qquad \text{(D14)}$$

and the constant, x_0, will be determined later.

For $t >> t_0$,

$$x_m(t) = l_{ox} - x_0 \ln(t/t_0)), \tag{D15}$$

$$v = x_0/t, \tag{D16}$$

and, for $t << t_0$,

$$v = x_0/t_0. \tag{D17}$$

The last equation states that, for small t, the velocity of the front is constant. On the other hand, the annealing process, as a tunneling process, depends on the distance from the interface. This means that x_0 is of the same order of magnitude as the distance between the molecular layers of the crystal. It appears that the annealing front involves several molecular planes and the space value of the front is likely equal to x_0. Also, t_0 is a time of annealing inside this front, when the distance to the interface is constant.

In this case, the net charge distribution can be observed in the form (see Fig.14):

$$p(x, t) = p_0/\{\exp[(x - x_m)/x_0] + 1\}. \tag{D18}$$

We can also calculate the rate of charge annealing:

$$dp/dt = p_0 \exp[(x - x_m)/x_0]/\{\exp[(x - x_m)/x_0] + 1\}2\, d(x_m/x_0)/dt. \tag{D19}$$

This function has a critical point at $x = x_m$ and

$$dp(x_m)/dt = p_0\, d(x_m/x_0)/dt = p_0[x_0/(t + t_0)]. \tag{D20}$$

Using a step function for the charge distribution, as in Eq.(D12), we have

$$p(x, t) = \begin{cases} p_0, (x_m - x) >> x_0 \\ 0, (x - x_m) >> x_0. \end{cases} \tag{D21}$$

or

$$p(x, t) = \begin{cases} p_0, x < x_m \\ 0, x > x_m. \end{cases} \tag{D22}$$

Substituting Eq.(D22) into Eq.(D7) and assuming that $p_0 = p\Delta D$, where p is a coefficient, we obtain

$$\Delta V(t) = -(1/\varepsilon_0\varepsilon)\int_0^{x_m} dx \int_0^{x} p_0\, dx' \text{ and}$$

$$\Delta V(t) = -(1/2\varepsilon_0\varepsilon)\, p_0(x_m)^2, \text{ or } \Delta V(t) = -(1/2\varepsilon_0\varepsilon)\, p[1 - x_0 \ln(t)]^2\Delta D. \qquad (D23)$$

When $\ln(t) << l_{ox}/x_0$, Eq.(D23) becomes

$$|\Delta V(t)| = [C - A \ln(t)]\Delta D,$$

where $C = (1/2\varepsilon_0\varepsilon)pl_{ox}^2$, $A = (1/\varepsilon_0\varepsilon)pl_{ox}x_0$ and $C/A = l_{ox}/2x_0$. We can calculate the total annealing time from Eq.(D23):

$$\ln(t_a/t_0) = l_{ox}/x_0.$$

If $l_{ox} = 50$ nm, $x_0 = 1.5$ nm and $t_0 = 10^{-4}$ sec, we obtain $t_a = 3.0 \times 10^{10}$ sec. For single-channel (we assume that hole traps can be different types, as we will see later from the experimental data) annealing, we can derive the equation for R(t):

$$R(t) = C - A \ln(t) + (A^2/4C) \ln^2(t). \qquad (D24)$$

This solution is crucial for long-term annealing. For simultaneous irradiation and annealing, the third term of Eq.(D24), $\ln^2(t)$, enables us to extend a description of annealing beyond the critical time region, $\ln(t_c) = C/A$, as in Fig.15 The new critical time can be calculated from:

$$\ln(t_c) = 2C/A. \qquad (D25)$$

Using Eq.(D22) and (D7), we can also relate the change in the threshold potential to the total initial charge, $Q = p_0 l_{ox} S$,

$\Delta V(t) = -(1/2\varepsilon_0\varepsilon)\, Qx_m^2(t)/l_{ox}S$, or, assuming uniform charge distribution, to the charge at time, t:

$$\Delta V(t) = -(1/2\varepsilon_0\varepsilon)\, Q(t)\, x_m(t)/S, \text{ where } Q(t) = p_0 S x_m(t).$$

Using Eq.(D9), we can obtain for our uniform charge distribution

$$\Delta V/\Delta V_0 = x_m^2(t)/l_{ox}^2, \qquad (D26)$$

where ΔV_0 is the initial shift, $-(1/2\varepsilon_0\varepsilon)p_0 l_{ox}^2$.

Eq.(D26) gives us the same response function, R(t),

$$\Delta V/\Delta V_0 = 1 - (2x_0/l_{ox}) \ln(1 + t/t_0) + (x_0^2/l^2) \ln^2(1 + t/t_0).$$

For the long-term approximation, we can derive

$$\Delta V(t) = -(p_0 l^2/2\varepsilon_0\varepsilon)[1 - (2x_0/l_{ox}) \ln(t) + (x_0^2/l_{ox}^2) \ln^2(t).$$

Simultaneous Irradiation and Annealing

The term $\ln^2(t)$, in Eq.(D24), which is non-linear with log(t), enables us to extend the description of radiation response to the case of simultaneous irradiation and annealing beyond the critical time point, $\ln(t_{c1})$ up to time, $\ln(t_{c2}) = 2C/A$.

We can also easily integrate Eq.(D24) according to Eq.(11) and obtain a more precise description of the radiation response for simultaneous irradiation and annealing:

$$\Delta V/\dot{D}t = -(A + C + A^2/2C) + (A + A^2/2C)\ln(t) - (A^2/4C)\ln^2(t). \qquad \text{(D27)}$$

In this case, the value of the balance time, where equilibrium between the damage introduction rate and the annealing rate occurs, can be derived, determining the balance value of the response:

$$d(\Delta V/\dot{D})dt = -C + A\ln(t_b) - (A^2/4C)\ln^2(t_b) = 0, \text{ and}$$

$t_b = \exp(2C/A)$. The balance value of the response is derived as

$$\Delta V_b = -\dot{D}(A^2/2C)\exp(2C/A). \qquad \text{(D28)}$$

DEVELOPMENT OF THE TEST

Experimentally, annealing at elevated temperatures is known to be a factor which enables a number of different devices to recover their operating characteristics after radiation damage faster than at normal temperatures both during and after irradiation.

It should be noted that, while simultaneous irradiation and annealing are taking place, the device parameters will continue to change until an equilibrium condition is reached between the damage introduction rate and the annealing rate, determining the constant equilibrium value of the shift in the parameter.

In the foregoing part, we have developed a linear response theory (LRT) to be applied to predicting the radiation/annealing response, i.e., the deviation of sensitive parameters, for any type of device which exhibits radiation response and time-dependent recovery in any parameter, for long-term (several months or years), low- and high-rate radiation environments. The LRT developed here does not depend on the device fabrication technology and can predict the equilibrium value of the shift in any parameter if the response is linear with dose and dose rate. In the other case, we have developed a non-linear approach, which can make predictions by calculation and by approximation of data, as shown in Figs.6, 7 and 8.

Thus, to develop a program and short-term (several hours or days) test procedure for making predictions for long-term annealing, we need to experimentally determine a number of constants in this theoretical model. We need to construct a new linear response function (LRF) for the very long-term region. At this point, our LRF can only give us an estimate of the long-term response. To develop the LRF for the long-term region, we need to compress the radiation/annealing process from several years in real time to a few hours or days in the laboratory. This time compression can be achieved if we subject the device to elevated temperatures.

From these tests at elevated temperatures, we shall determine the temperature dependence of the constants and the LRF behavior in the very long-term region at room temperature. Using approximations of radiation response for various dose rates in the non-linear case and the LRT result, we can make predictions of the very long-term radiation/annealing response of devices of any technology at any temperature.

1. Compression in time.

As has been shown in many experimental works[1, 10, 11, 12, 17, 20, 21], an elevated-temperature environment enhances annealing processes by decreasing the lifetime of trapping sites in insulators, such as SiO_2, increasing the probability of tunneling processes and decreasing thermal activation energy for trapping sites for MOS devices.

The elevated-temperature technique is therefore a very basic tool for the time compression of long-term processes for short-term observation in the laboratory.

a) Pure annealing.

As mentioned in the foregoing part, we have chosen to use the shift in threshold potential, V(t), for MOS ICs as the sensitive parameter, although the LRT method allows us to use any parameter which is affected by radiation.

We then obtain a family of experimental curves per unit dose at various temperatures of the form:

$$\Delta V(t)/D = -C + A \ln(1 + t/t_0),$$

as shown in Fig.16, or in the form from Fig.15:

$$\Delta V(t)/D = -C + A \ln(1 + t/t_0) - (A^2/4C) \ln^2(1 + t/t_0),$$

Note that the experimental curves of $\Delta V(t)$ per unit dose at various temperatures intercept each other at the an ordinate value equal to -C and at an abscissa value equal to $\ln(t_0)$. In this way, we can determine all the LRT parameters. The temperature dependence of the parameters can also be estimated from the family of experimental curves. According to the existing experimental data, we assume that the parameter A is strongly dependent on temperature.

For the pure annealing case, measurement of the shift of the threshold potential at large times, i.e., on the "tail" of the curve, is not possible because of limits in the accuracy of voltage measurements.

b) Simultaneous irradiation and annealing.

In an analogous manner, we can obtain a family of curves of $\Delta V(t)$ and $\Delta V(t)/D(t)$ at various temperatures, as shown in Fig.17.

We must explain that the similarity of the curves in Figs.16 and 17 is due to a theoretical manipulation. The difference between them is that, in Fig.16, $\Delta V(t)$ for pure annealing is divided by total impulse dose, $D = \dot{D}\Delta t$ (see Eqs.(4) and (5)), but in Fig.17, $\Delta V(t)$ for simultaneous irradiation and annealing is divided by instantaneous total dose, $D = D(t)$ (see Eqs.(13 and (14)). This trick is important because it permits analysis of experimental data for simultaneous irradiation and annealing conveniently and directly. To prove this, we can transform any experimental curve of the shift in the threshold potential for simultaneous irradiation and annealing into linear dependence on log(t) by dividing the values by the instantaneous total dose (or

the instantaneous time value if the dose rate is constant), as was done with experimental data[25] and shown in Figs.24 and 25.

In the previous paragraph, one method to determine the LRF parameters was shown. To determine the LRF constants and their temperature dependence, we also intend to use the experimentally-determined temperature-dependence curves of $\Delta V(t)$ which can be observed in Figs.16 and 17 for both pure annealing and simultaneous irradiation/annealing.

The determination of the LRF constants and their temperature dependence is necessary because we need:

- to estimate the critical region, i.e., the long-term region, where the LRF changes its behavior and the value of the critical time, t_c; we can determine the value of the critical time graphically by the LRF intersection with the abscissa;

- to determine the "time compression rate" (TCR, the coefficient of time compression, using critical time values and temperature dependence of the time for half recovery) and to choose the temperature needed to compress the time of a test;

- to calculate the values of the required test time at elevated temperatures, using the TCR;

- to determine the LRF constants for the long-term region by extrapolation of values of constants determined at elevated temperatures to room temperature;

- to determine the LRF for the long-term region at elevated temperatures (the critical time region, t_c, in Figs.16 and 17), then to extrapolate the LRF to room temperature and calculate the response if the radiation response is linear with respect to dose and dose rate.

2. Determination of LRF constants

a) Pure annealing.

To determine the constants A, C, and t_0, we expand Eq.(7) in a power series:

$$R(t) = -C + A \ln(1 + t/t_0) = -C + A(t/t_0) - (A/2)(t/t0)^2 + (A/3)(t/t_0)^3 - \ldots \qquad (E1)$$

The regions of the curve of Eq.(7), where the terms of this expansion are to be fitted are seen in Fig.18.

It was also shown in the foregoing part that we can determine A immediately, since it is the slope of a straight line, the response function, R(t), plotted vs. ln(t). Assuming C is constant, the points of interception of the family of R(t) curves at various temperatures for pure annealing, as shown in Fig.16, gives us the value of $\ln(t_0)$. Therefore, C and t_0 can be separated and determined from the coordinate of the interception, $[-C - A \ln(t_0)]$. We assume that C is temperature-independent, as the experimental study[22] shows.

The determination of all the LRF constants from the family of curves for pure annealing seems reliable, but errors in measurement of the shift in the threshold potential in the long-term region can become comparable to the value of the potential shift itself. Such a difficulty can be solved by using simultaneous irradiation and annealing data divided by instantaneous dose, as shown in Figs.24 and 25.

Also, as will be shown later, we can determine all the constants from the temperature dependence of the time for half recovery and the temperature dependence of the critical time.

b) Simultaneous irradiation and annealing

To determine A, C, and t_0, we expand Eq.(12) in a power series in (t/t_0) as follows:

$$\Delta V/D = -C + [A(t/t_0)]/2 - [A(t/t_0)^2]/6 - [A(t/t_0)^3]/12 - \ldots \qquad (E2)$$

We will obtain a family of experimental LRF curves, as shown in Fig.16, for various temperatures for both pure annealing and simultaneous irradiation and annealing. The LRF constants and their temperature dependence will be established.

In order to demonstrate the possibility of determining the LRF constants in this way, we obtained the experimental data shown in Figs.25 and 26. N- and p-channels of an RCA CD4007 integrated circuit were given impulse doses of 1 MeV electrons up to 10 kRads. As a source of electrons (up to 1.6 MeV), we used the 2 MeV Van de Graaff accelerator of the NASA/Goddard Space Flight Center Radiation Facility at Greenbelt, MD. Radiation dose was measured with radiochromic films, using a FWT Technology film reader. Doses are given in Rads-Si. The points in Figs.25 and 26 are the experimental data and the solid lines represent Eq.(E2).

3. Determination of the time for half recovery, $t_{1/2}$, for various temperatures and the "Time Compression Rate" (TCR).

An additional method to determine all the LRF constants, as shown in Fig.19, is to plot the dependence of the time required for half recovery vs. the reciprocal of temperature. The time for half recovery is supposed to be the time needed to anneal half of the quantity of damage in the sensitive parameter in the pure annealing case.

Experimental data of the time of half recovery vs. reciprocal of temperature are shown in Fig.19.
According to Eqs.(13) and (6), we can obtain:

$$t_{1/2} = (t_0 t_r)^{1/2} \exp[(C-A)/2A], \tag{E3}$$

where $t_{1/2}$ is the time for half recovery and t_r is the time at which irradiation ceases.

Using Eqs.(16) and (8), we can estimate the character of the temperature dependence of the time of balance - the equilibrium time, t_b, as follows:

$$t_b = t_0 \exp(C/A),$$

and, if the slope, A, of the response function is equal to b + aT, where a and b are constants, T is the temperature and $b << aT$,

$$\ln(t_b) = \ln(t_0) + (C/a)(1/T) \text{ and} \tag{E4}$$

$$\ln(t_{1/2}) = \ln[(t_0 t_r)^{1/2} \exp(-1/2)] + (C/2a)(1/T). \tag{E5}$$

Terrell et al.[22] have presented experimental data of temperature dependence of the time for half recovery plotted against the reciprocal of temperature. We can compare these data to our Eq.(E5). Setting $\Delta T = 50^oC$ gives us $t_{1/2}/t'_{1/2} = 10$.

To find the equilibrium time, t_b, we used the time for half recovery, Eq.(18),

$$t_b \propto (t_{1/2})^2. \tag{E6}$$

The temperature shift, $\Delta T = 50^o$, gives us approximately $t_b/t'_b = 100$.

We can also determine the time for half recovery, $t_{1/2}$, more conveniently from Eq.(6) for pure annealing:

$$t_{1/2} = t_0 \exp(C/2A), \text{ or, for } A = aT,$$

$$t_{1/2} = t_0 \exp[(C/2a)(1/T)]. \tag{E7}$$

We obviously have experimental confirmation of LRT efficiency, comparing Eqs.(E7) and (E5) with the experimental result[22].

For a practical test procedure, it would be helpful to determine the time required for one-third recovery, etc.

The "Time Compression Rate" (TCR) for the critical-equilibrium time region could be determined from the extrapolation as is shown in Fig.19. We can thus calculate the

required test time at various temperatures to simulate the flight time. The calculation is done using Eqs.(E7) and (E4) as follows, if T'>T:

$$t_b(T) = t_b(T')[t_{1/2}(T)/t_{1/2}(T')]^2 \text{ or}$$

$$t_b(T) = t_b(T') \exp\{[(T-T')/TT']C/a],$$

i.e., time values in the long-term region can be calculated as follows:

$$t(T) = t(T') \exp(C/a)(1/T - 1/T').$$

From this equation,

$$TCR = \exp[(C/a)(1/T - 1/T')]. \qquad \text{(E8)}$$

4. The test procedure

The test procedure is a product of the linear response theory developed here applying the procedure for determination of LRF constants and the non-linear approach (as in Figs.7, 8, 9 and 10). The main goal of this program is to develop short-term (several hours or days) test procedures, accelerating annealing at elevated temperatures, for linear radiation response with respect to dose and dose rate, or increasing the dose rate for non-linear response with respect to dose rate, for making predictions for long-term (several months or years) annealing in space.

In order to conduct the test, the test procedure program would consist of:

a) Determination of all constants of the LRF, taking into account the form of the LRF equation, $R(t) = -C + A \ln(1 + t/t_0)$ (or a sum of similar equations, as we will show later with experimental data, remembering the "tail", $-(A^2/4C) \ln^2(1 + t/t_0)$, from Eq.(D19), which is sufficient for the long-term region). The LRF constants are:

- the characteristic time of annealing, t_0,
- the intensity of annealing, A, and
- the damage introduction rate, C,

which are obtained both from experimental data of pure annealing and simultaneous short-term irradiation and annealing data. To calculate the value of equilibrium, i.e., the value of the long-term region, when $t >> t_0$, we can apply the complete equation, Eq.(D19):

$$R(t) = -C + A \ln(t/t_0) - (A^2/4C) \ln^2(t/t_0).$$

b) Calculations performed in order to estimate the instant in time (the "critical time", $t_c = t_0 \exp(C/A)$), at which the annealing begins to change its behavior. For example, pure annealing of the shift in the threshold potential has been observed to deviate from linearity with respect to the logarithm of annealing time.

The same calculations determine when simultaneous irradiation and annealing can be expected to reach equilibrium:

$$t_b = t_0 \exp(C/A) \text{ or } t_b = t_0 \exp(2C/A) \text{ from Eq.(D21).}$$

c) The value of the balance of the shift in the sensitive parameter, for example, the shift in the threshold potential:

$\Delta V = -A\dot{D}t_0 \exp(C/A)$ (the equilibrium value) or, more precisely,

$\Delta V = -\dot{D}(A^2/2C)t_0 \exp(2C/A)$, would be estimated.

d) Extrapolation. Since thermal time compression is applied, the test data would be obtained at high temperatures. These data would be extrapolated to room temperature for making predictions by using the temperature dependence of the LRF constants.

Since the elevated-temperature technique enables us to compress the duration of the radiation test from several years at room temperature to a few hours or days at elevated temperatures, the experimental radiation/annealing occur as a family of experimental curves of the shift in the sensitive parameter, for example, in the threshold potential per unit dose at various temperatures, in the form:

$\Delta V(t)/D = -C + A \ln(1 + t/t_0)$ and

$\Delta V(t)/\dot{D}t = A(1 + t_0/t) \ln(1 + t/t_0) - (A + C)$ or, in complete form:

$\Delta V(t)/D = -C + A \ln(1 + t/t_0) - (A^2/4C) \ln^2(1 + t/t_0)$ and for $t >> t_0$,

$\Delta V/\dot{D}t = -(A + C + A^2/2C) + (A + A^2/2C) \ln(t/t_0) - (A^2/4C) \ln^2(t/t_0)$,

where A, C and t_0 are the constants of the LRF and dose rate $\dot{D} = dD/dt$,

for both pure annealing and simultaneous irradiation and annealing.

Thus, this practical procedure for development of the radiation damage/annealing test consists of the following steps in order:

- to determine dose limit for linearity of IC radiation response with respect to dose and dose rate;

- to obtain the radiation damage/annealing data at various elevated temperatures for the short-term and long-term regions;

- to determine the form of the LRF, the LRF constants and their temperature dependence for the short- and long-term regions;

- to estimate the long-term region, i.e., the theoretical and experimental value of the critical time, t_c, in the long-term region for various temperatures, when the LRF changes its behavior; we expect to obtain a value equal to $t_0 \exp(C/A)$;

- to determine the theoretical and experimental value of the time for half recovery, $t_{1/2}$, for various temperatures; we expect to obtain a value equal to $t_0 \exp(C/2A)$ and a linear dependence on the reciprocal of temperature which leads to a reasonably linear temperature dependence of the constant A;

- to determine the "time compression rate" (TCR, the coefficient of time compression) for the long-term region, i.e., the critical time region, and to choose the temperature to compress the test time; we expect to confirm the theoretical quadratic dependence of the critical or balance time, $t_c = (1/t_0)(t_{1/2})^2$ which, as was shown experimentally gives us a TCR equal to 100 when $\Delta T = 50^oC$[22];

- to calculate the TCR for required test time to simulate spaceflight time;

- to calculate the radiation response for the required test time;

- to determine the IC's response under increased dose rate (for shortened test time) for various dose rates if the response is non-linear with dose rate;

- to extrapolate the values of the radiation response at the increased dose rates (see Fig.10), to the space dose rate.

This practical program enables us to construct the annealing test to make predictions of radiation response of MOS devices for long-term (months and/or years) operations.

EXPERIMENTAL APPROACH

We have good evidence that our approach using LRT is more than just theory. We can actually obtain the necessary experimental data, introduce our linear response theory, evaluate the LRF constants and predict the radiation response by extrapolation of the values of the LRF constants from elevated temperatures to normal room-temperature operation.

In observing the experimental results and theoretical models, we see that we must describe the process of annealing through tunneling in a more complex way than often theoretically described. The experimental results point to at least two different tunneling models. We can actually presume many more channels of annealing.

In Fig.21, we can see the experimental results of pure annealing.

It is clear, especially for 150°C, that we have at least two annealing channels:

1) the first, from the beginning of the curve up to 1 sec.;

2) the second, from 1 sec. to the of measurement of the experimental region.

We believe that annealing is taking place through two tunneling modes, not one as in the McLean model. As shown in Fig.13, the tunneling modes are:

(i) from electron levels above the Si conduction band to a temperature-dependent excited (because of the parallel spin alignment of the electrons) triplet hole trap state with energy about 1 - 1.35 eV above the Si conduction band, and

(ii) from levels below the Si valence band to a temperature-dependent ground (singlet, because the two electron spins are antiparallel in the same orbital) hole trap state with energy about 3 - 3.5 eV above the SiO_2 valence band (with 9 eV SiO_2 bandgap).

We may also have thermal annealing by thermally excited electrons from the valence band of the oxide[25]. We can therefore assume many more channels of annealing and our main approach using LRT does not depend on it, as we will explain later.

From these experimental data, we determined the temperature dependence of the quantity of hole traps distributed between the excited and ground states, i.e., the value of the LRF constants, C_1', C_2', A_1, A_2 and their temperature dependence as seen in Fig.22. The critical time and time compression rate temperature dependence are shown in Fig.23 and the form of the LRT functions (Fig.21) is given by:

$$R(t) = R_1(t) + R_2(t), \text{ where } R_1(t) = -C'_1 + A_1 \ln(t)/[1 + (t/t_c)^2],$$

$$R_2(t) = -C_2' + A_2 \ln(t).$$

We assume that $C' \sim N$, where N is the density of charged states. According to the theoretical thermal model[26], we have:

$$N = k(T)^{3/2},$$

where k is a coefficient and T is temperature (°K). Comparing out results with this model, we observe good agreement, as seen in Fig.22.

We have assumed that the time units are in seconds. For convenient treatment of the experimental data and easy determination of the initial shift, we use a new term, the "primary time", t', equal to 10^{-4} seconds,

$$R_1(t') = -C_1' + A_1 \ln(t') = -C_1 \text{ and}$$

$$R_2(t') = -C_2' + A_2 \ln(t') = -C_2.$$

Using such a technique, we can treat any experimental data obtained at elevated temperatures for both pure annealing (for an impulse dose) and simultaneous irradiation and annealing (dividing experimental values by instantaneous total dose), derive equations, determine constants, time reduction coefficients and required test time for elevated temperatures. Then we can make predictions of annealed-equilibrium radiation damage for spaceflight time values directly from the experimental curves or calculate the required value using the equation for this time region.

Despite the seeming complexity in dealing with many annealing channels, the LRT approach can manage each portion of the annealing curve if the radiation response is linear with respect to dose. Principal attention should be directed to relating the portion of the curve at one temperature to that at another temperature in order to determine the LRF constants for the latest or necessary part of the annealing curve and to calculate the value of the radiation response,i.e., the shift in the threshold potential, for a certain time value and at the spacecraft temperature corresponding to the related value at the elevated test temperature.

Let us examine the experimental data obtained at room temperature (25°C) and at elevated temperatures, i.e., 75°C, 125°C and 150°C, which are shown in Fig.21. We can immediately determine at least two straight line portions of each curve and the LRF constants. Fortunately, we can also see that the annealing at 150°C is almost complete. As can be seen, the annealing at the highest temperature is nearly complete at 10^3 seconds. The annealing for the corresponding segment of the curve at 125°C would require 10^9 seconds to go to completion, or close to 30 years. The result of the treatment of the experimental data of the same segment of the curves for 25°C and 75°C is less reliable because of a lack of statistics, but the approximate value of the time for completion of annealing would be about 10^{16} seconds. As is shown, the time interval is significant for any long-term calculations. Thus such experimental data can give us the law of approximation for the LRF constants (Fig.22) and the time compression rate (Fig.23). Knowing the spaceflight time, we can calculate the test time for elevated temperatures, choose the right time region and the essential part of the annealing curve. We can then determine the value of the shift of the parameter for the chosen time at the elevated temperature and approximate this value to the value at room temperature, using the previously-obtained LRF curves for various temperatures. We can directly calculate the prediction, using the the curves of the temperature dependence of the LRF constants, or the temperature dependence of the shift value. We can also determine the shift in the threshold potential using the

curve of the shift at the elevated temperature and the decreased value of the required test time from the graph.

Since the accuracy of the threshold potential measurement at the low-voltage region, where annealing is almost complete is low, we can use the experimental data for simultaneous irradiation and annealing divided by instantaneous dose, as shown in the foregoing theoretical part. Such an operation yields a similar straight line with respect to log(t) or a sum of such lines, as lines of pure annealing. Examples of the experimental curves divided per instantaneous dose are shown in Figs.24 and 25. The treatment of such experimental data would be almost the same as for pure annealing.

Although the experimental data are not statistically complete and were obtained for only four temperatures, this approach has nevertheless given us the form and constants of the LRF for long-term regions close to 10^{16} seconds. These efforts to make predictions will be continued with more statistically complete experimental data.

CONCLUSION

This paper is a report of three years' effort in which we have seen great success in applying the proposed linear response theory to make predictions of the radiation response of ICs for long-term operation in space. The first experiments using the test procedure developed with LRT to obtain experimental data showed us the usefulness of the technique to produce predictions for very long-term operation (10^{16} sec.), at least for this device. The approach for making predictions of radiation response which is non-linear with respect to dose rate has also been demonstrated.

The theoretical result, based on the theoretical models of basic processes in the IC during irradiation, gives the complete equation of the radiation response, Eq.(D19), which could hardly be determined experimentally.

Although the LRT could not be applied for the non-linear case, we suppose that it can be used in the low-dose-rate space radiation environment along with our capability to determine the additional difference due to the non-linear effect. The quasi-linear approach and the method of extrapolation of data will help to determine this difference.

In addition, we should note:

1. different devices have different characteristics of radiation damage and annealing curves, but the linearity of the response with log(t) on each part of the curve is a permanent characteristic; the LRT can be easily applied for all such devices;

2. observing the theoretical models, we were interested only in hole-trapped charge; we did not concern ourselves with radiation-induced interface electron-trapped charge, because this charge buildup is not temperature-dependent. However, the LRT enables us to apply the LRF method in this case, if the linearity with dose is observed.

The experimental program to obtain the prediction of radiation damage for long-term space operation, using the LRT method LRT and the non-linear approach to different devices will be applied in the CRRES Ground Simulation Experiment.

REFERENCES

1) V. Danchenko, U.D. Desai, S. Brashears, J. Appl. Phys., Vol.39, No5, 2417(1968).

2) M. Simons, H.L. Hughes, IEEE Trans. Nucl. Sci., NS-19, 282(1970).

3) M. Simons, H.L. Hughes, Ibid., NS-18 106(1971).

4) D.H. Habing, B.D. Shafer, Ibid., NS-20 No.6, (1973).

5) G.F. Derbenwick, H.H. Sander, Ibid., NS-24, No.6, 2244(1977).

6) P.S. Winokur, Ibid., NS-29, No.6, 2102(1982).

7) P.S. Winokur, K.G. Kerris, L. Harper, Ibid., NS-30, No.6, 4326(1983).

8) P.S. Winokur, H.E. Boesch, Jr., Ibid., NS-28, No.6, 4088(1981).

9) V. Danchenko, U.D. Desai, S. Brashears, J. Appl. Phys., Vol.39, No.5, 2417(1968).

10) J.R. Schwank et al., IEEE Trans. Nucl. Sci., Vol.35, No.6, Dec. 1986.

11) F.B. McLean, Ibid., Vol.35, No.6, Dec. 1988.

12) V. Danchenko, P.H. Fang, S.S. Brashears, Ibid., NS-29, No.6., Dec. 1982.

13) F.B. McLean, "A Direct Tunneling Model of Charge Transfer at the Insulator-Semiconductor Interface in MIS Devices", Harry Diamond Laboratories, HDL-TR-1765 (Oct. 1976).

14) J.M. Terrell, T.R. Oldham, A.J. Lelis, J.M. Benedetto, IEEE Trans. Nucl. Sci., NS-36, Dec. 1989.

15) T.R. Oldham, T.R. Oldham, F.B. McLean, Ibid., NS-33, 1203(1986).

16) S. Manzini, A. Modelli, "ln(t) Dependence in Insulating Films on Semiconductors", pg. 112, J.F. Verwels and D.R. Wolters, eds., North-Holland, New York 1983.

17) A.J. Lelis, T.R. Oldham, H.E. Boesch, Jr., F.B. McLean, IEEE Trans. Nucl. Sci., NS-36, Dec. 1989.

18) J.H.Scofield, T.P. Dierr, D.M. Fleetwood, Ibid., Vol.36, No6, Dec. 1989.

19) D.B. Brown, W.C. Jenkins, A.H. Johnston, Ibid., Vol.36, No.6, Dec. 1989.

20) D.M. Fleetwood, P.S. Winokur, L.C. Riewe, R.L. Pease, Ibid., Vol;.36, No.6, Dec. 1989.

21) J.R. Schwank, F.W. Sexton, D.M. Fleetwood, M.R. Shaneyfelt, K.L. Hughes, M.S. Rodgers, Ibid., Vol.36, No.6, Dec. 1989.

22) J.M. Terrell, T.R. Oldham, A.J. Lelis, J.M. Benedetto, Ibid., NS-36, Dec.1989

23) F.B. McLean, H.E. Boesch, Jr., Ibid., Dec. 1989.

24) P.J. McWhorter, S.L. Miller, W.M. Miller, "Modeling the Anneal of Radiation-Induced Trapped Holes in a Varying Thermal Environment", Preprint of Sandia National Laboratories, 1990.

25) E.W. Enlow, R.L.Pease, MRC, W.E. Combs, D.G. Platteter, NWSC, NWSC Preprint, 1990.

26) S.M. Sze, "Physics of Semiconductor Devices", John Wiley & Sons, New York, 1981.

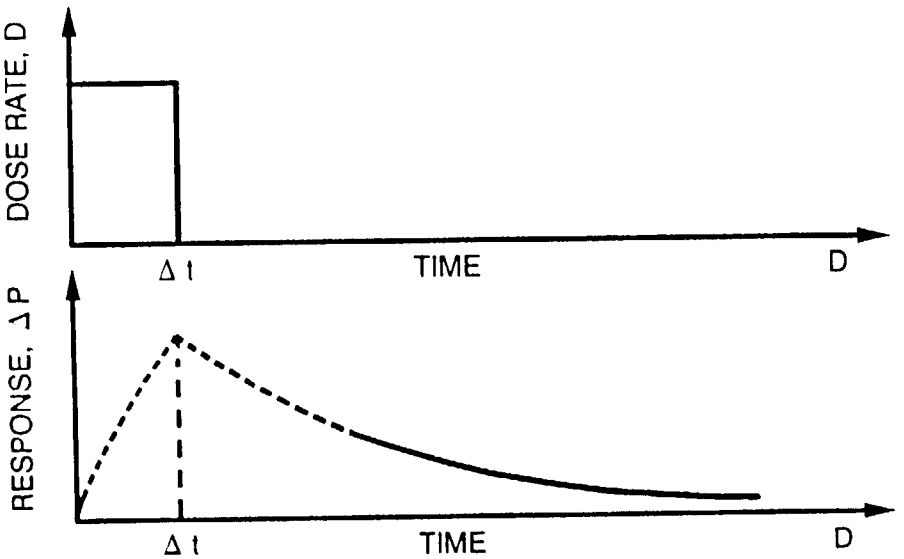

FIG. 1. Impulse dose, $D = D\Delta t$, and radiation response, ΔP, as function of time and dose.

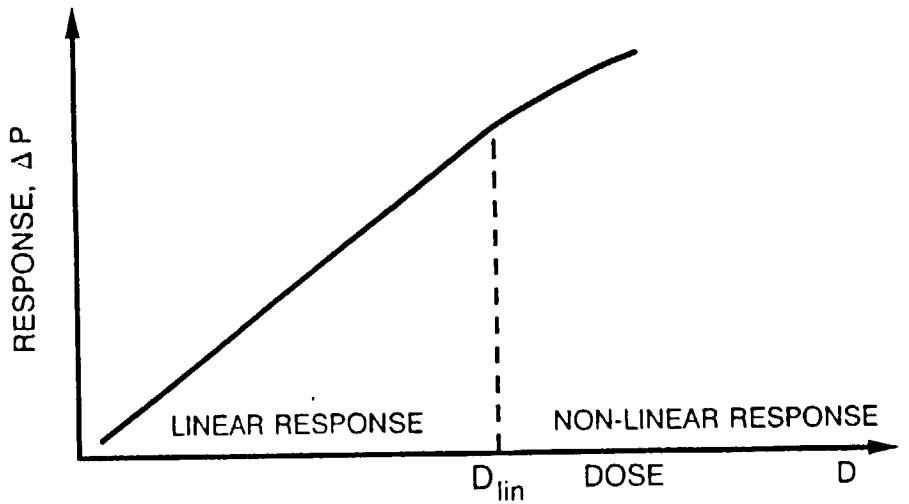

Fig. 2. Determination of the linear region. Response is measured at fixed moment, t.

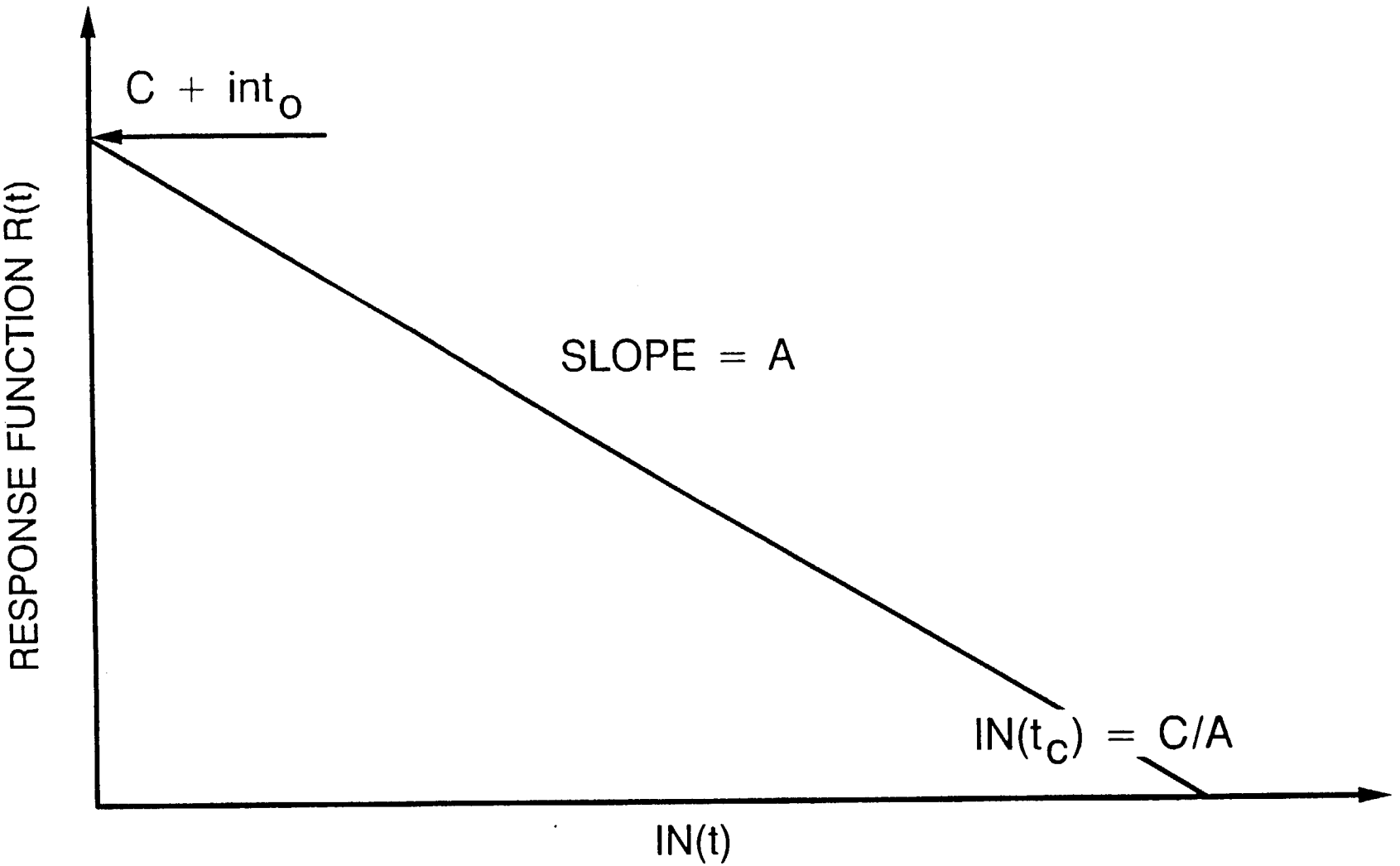

Fig 3. Linear response function and its constants

D25.001

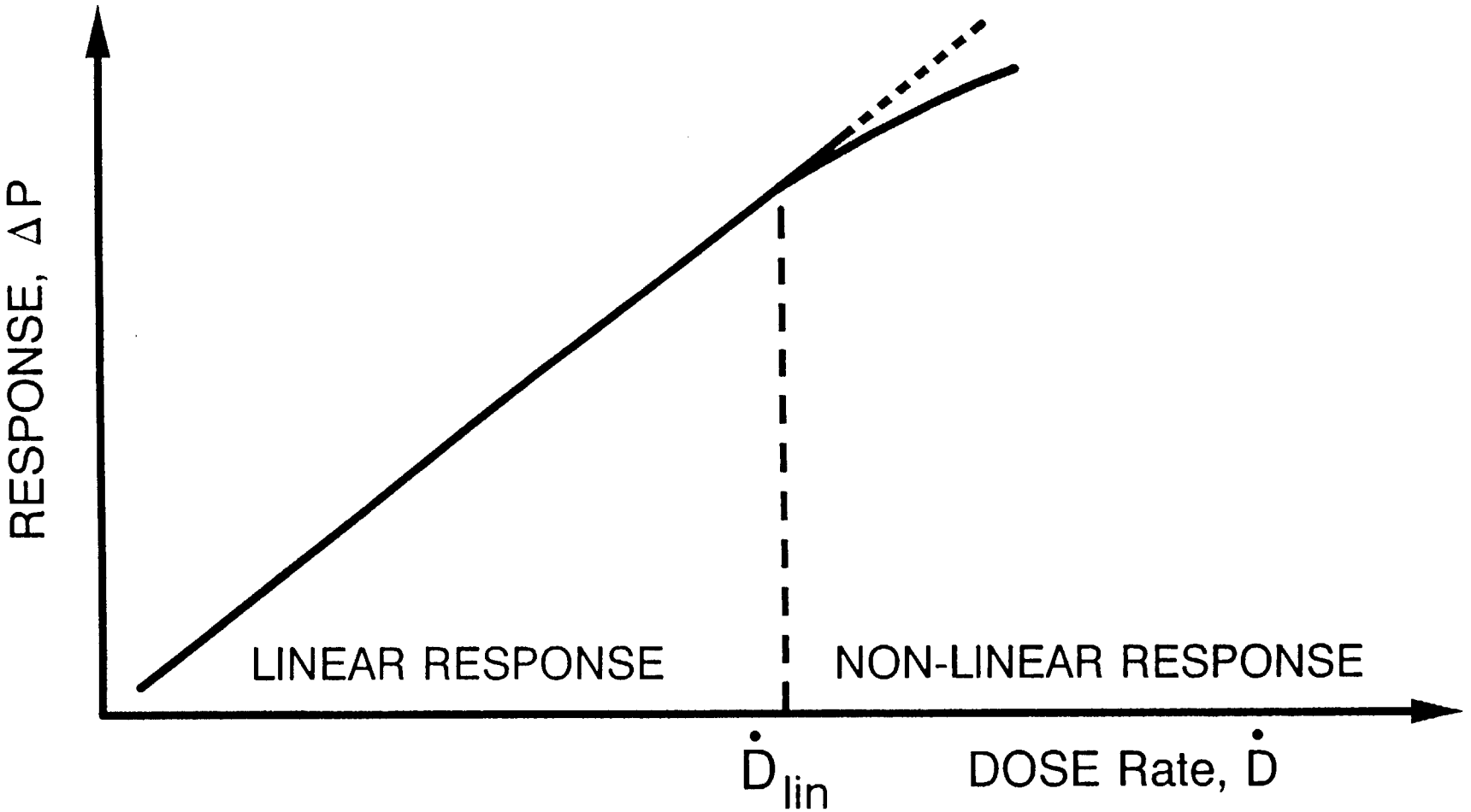

Fig. 4. Determination of a linear region, $\dot{D} < \dot{D}_{lin}$, in which the response ΔP is still linear.

D25.003

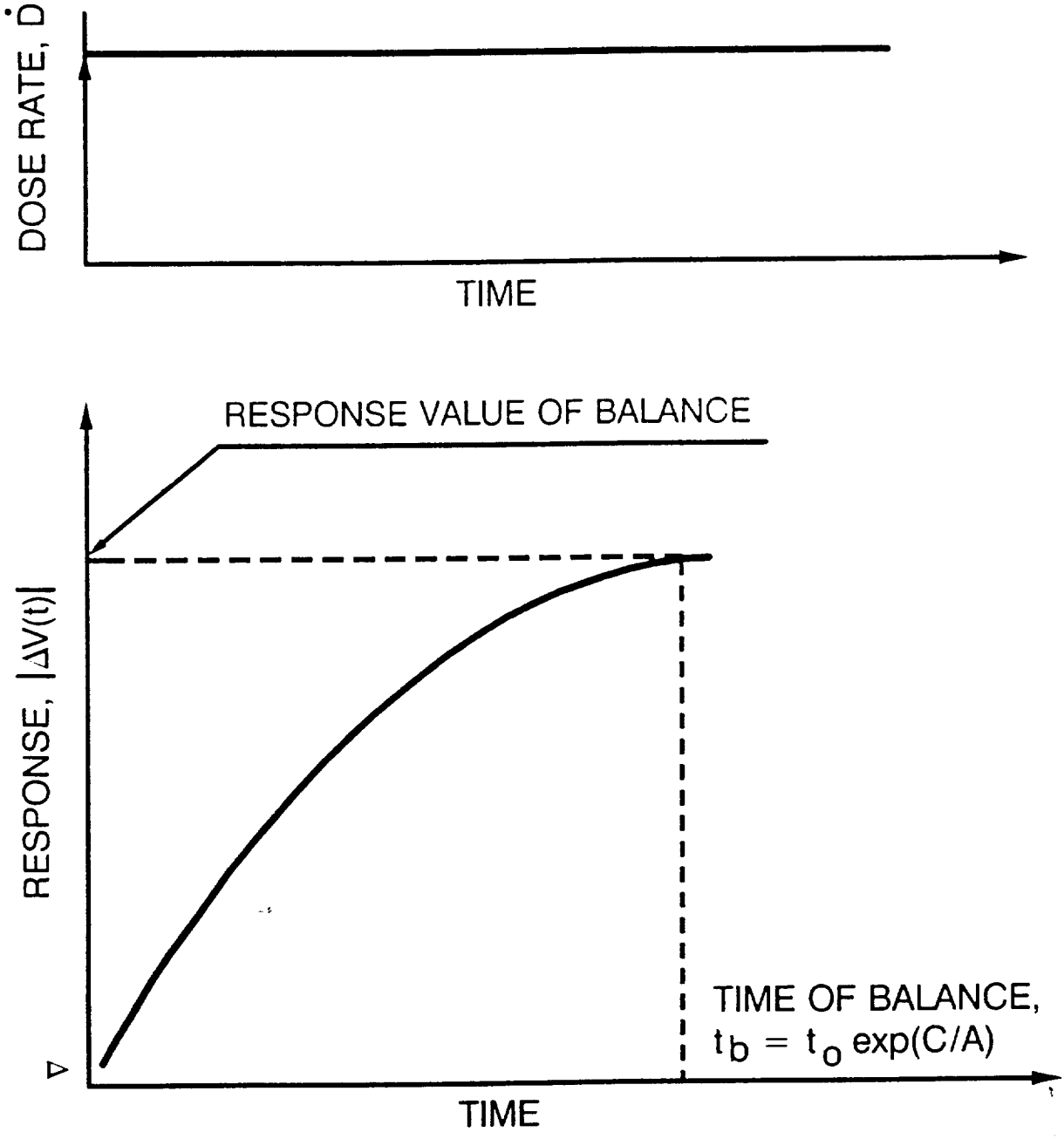

Fig. 5. Continuous irradiation and the shift in the threshold potential, V(t). The balance between the damage rate and annealing rate.

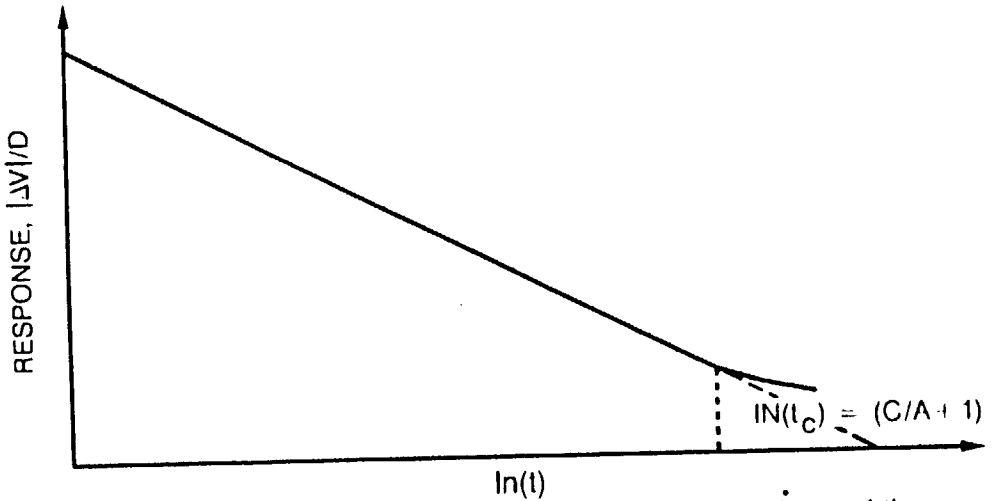

Fig. 6. The Shift, $[\Delta V]$, per unit current dose, $D = \dot{D}t$, and the time of deviation, t_d.

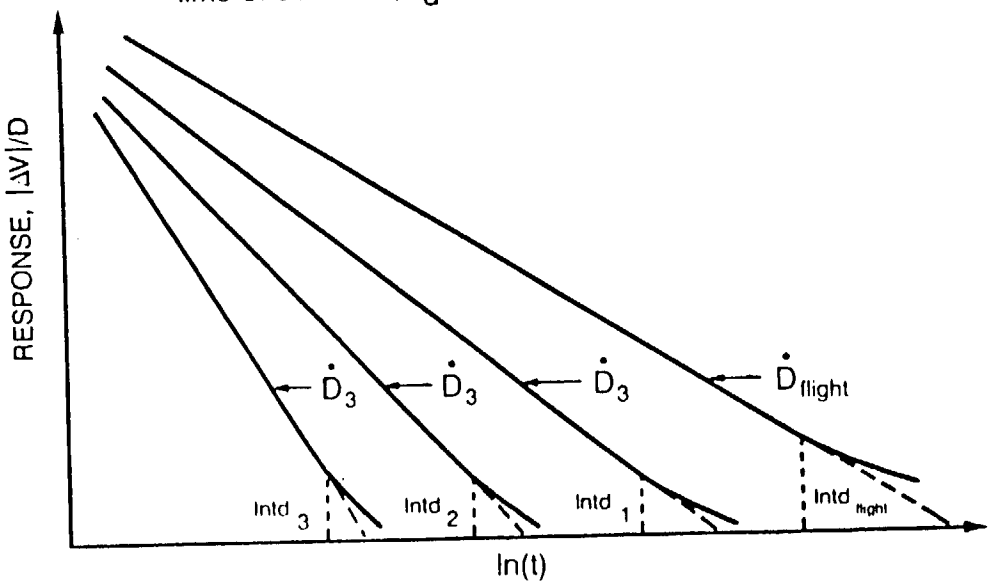

Fig. 7. Family of response curves for different dose rates, $D_1 < D_2 < D_3$.

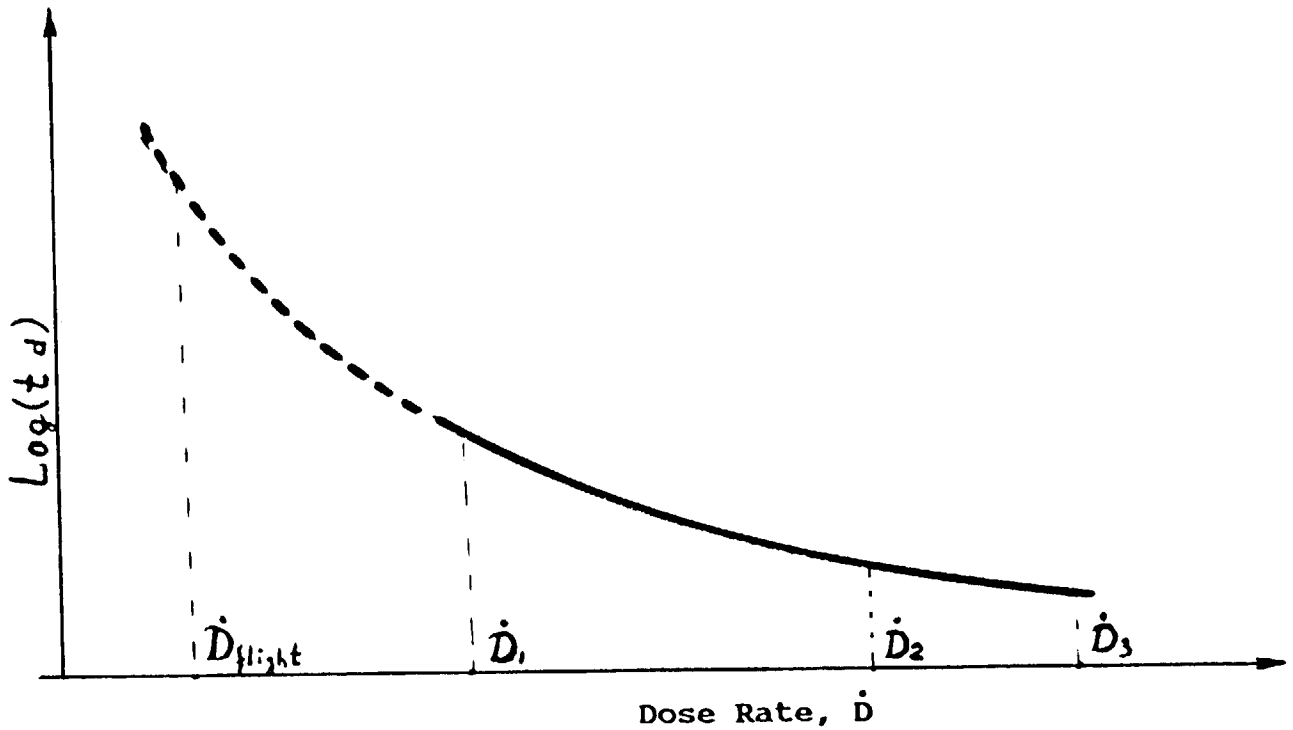

Fig.8. Extrapolation of data of values of the time of deviation in order to find out the time compression rate for the flight time for various dose rates.

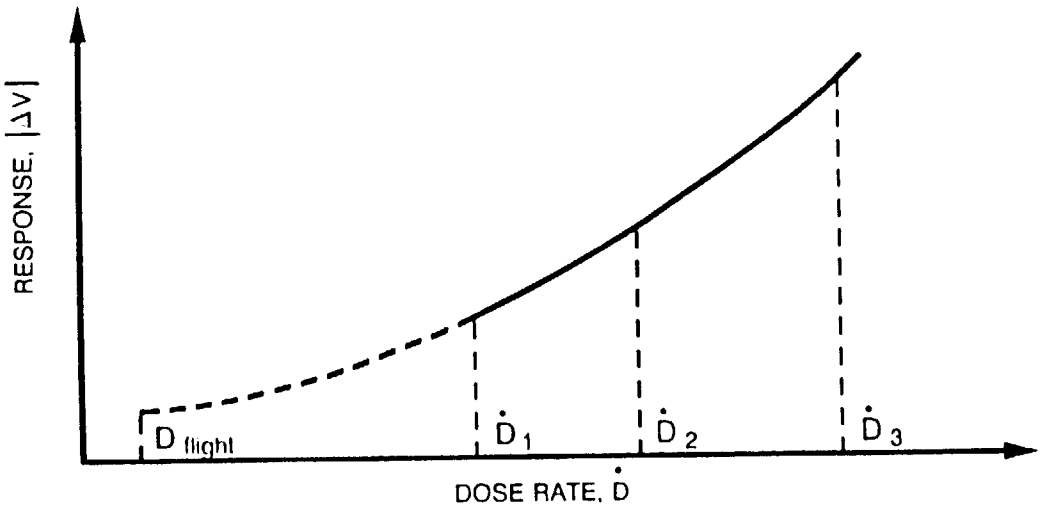

Fig. 10. Extrapolation of response data from increased dose rate to space-like dose rate.

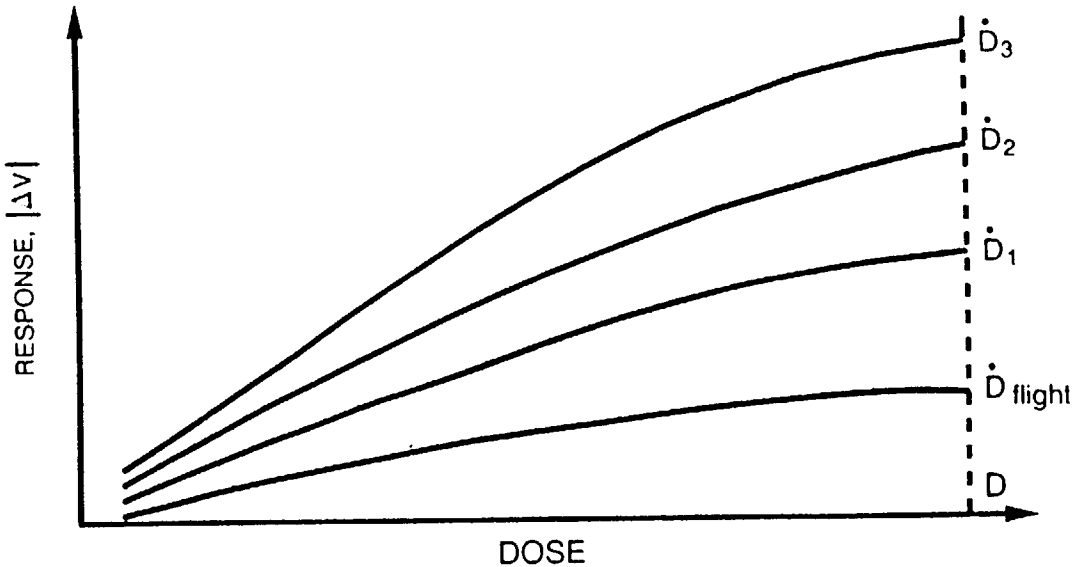

Fig. 9. Radiation response vs. accumulated dose from different dose rate.

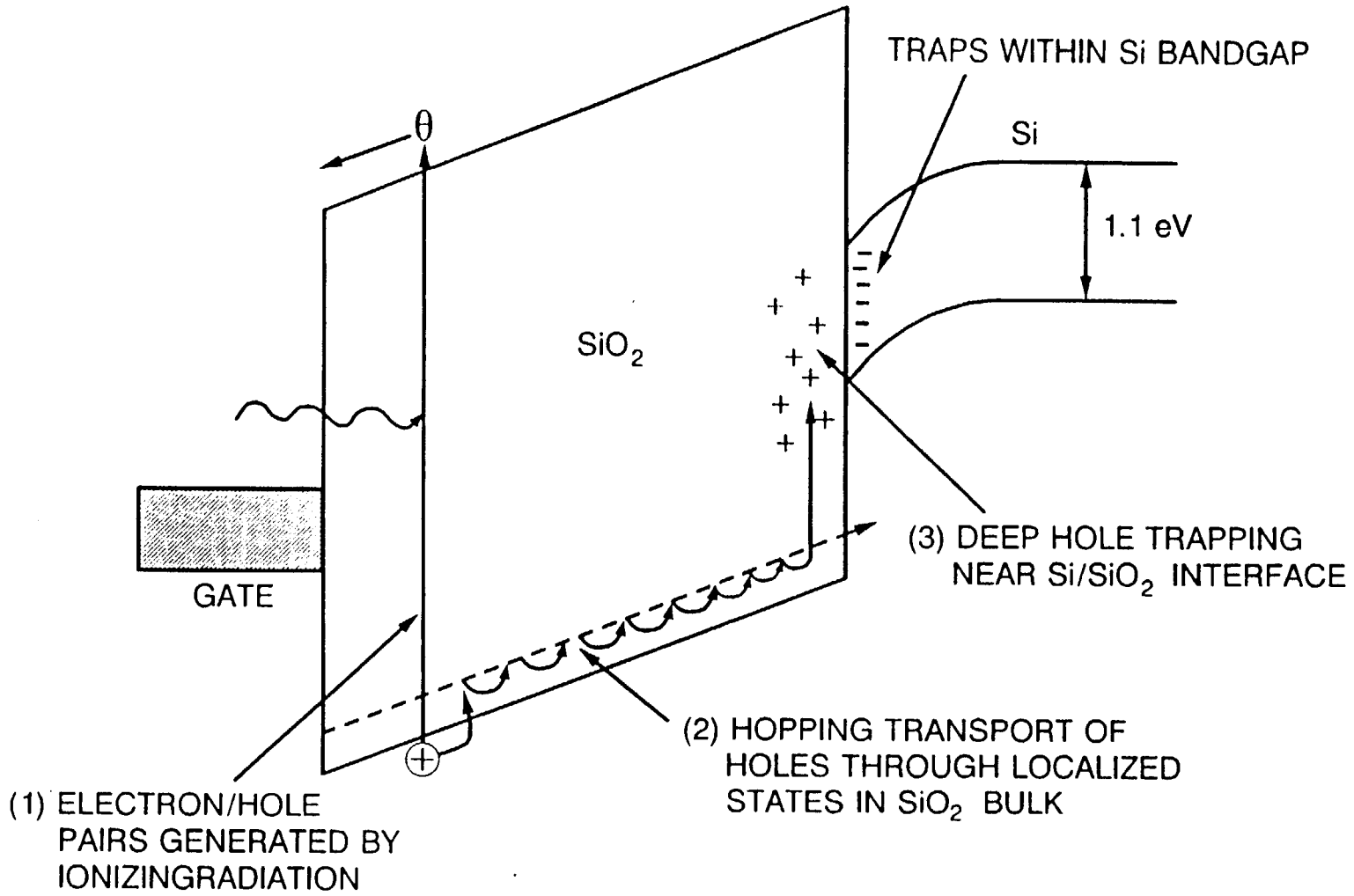

Fig. 11. Schematic of basic radiation effects in MOS structures

D25.008

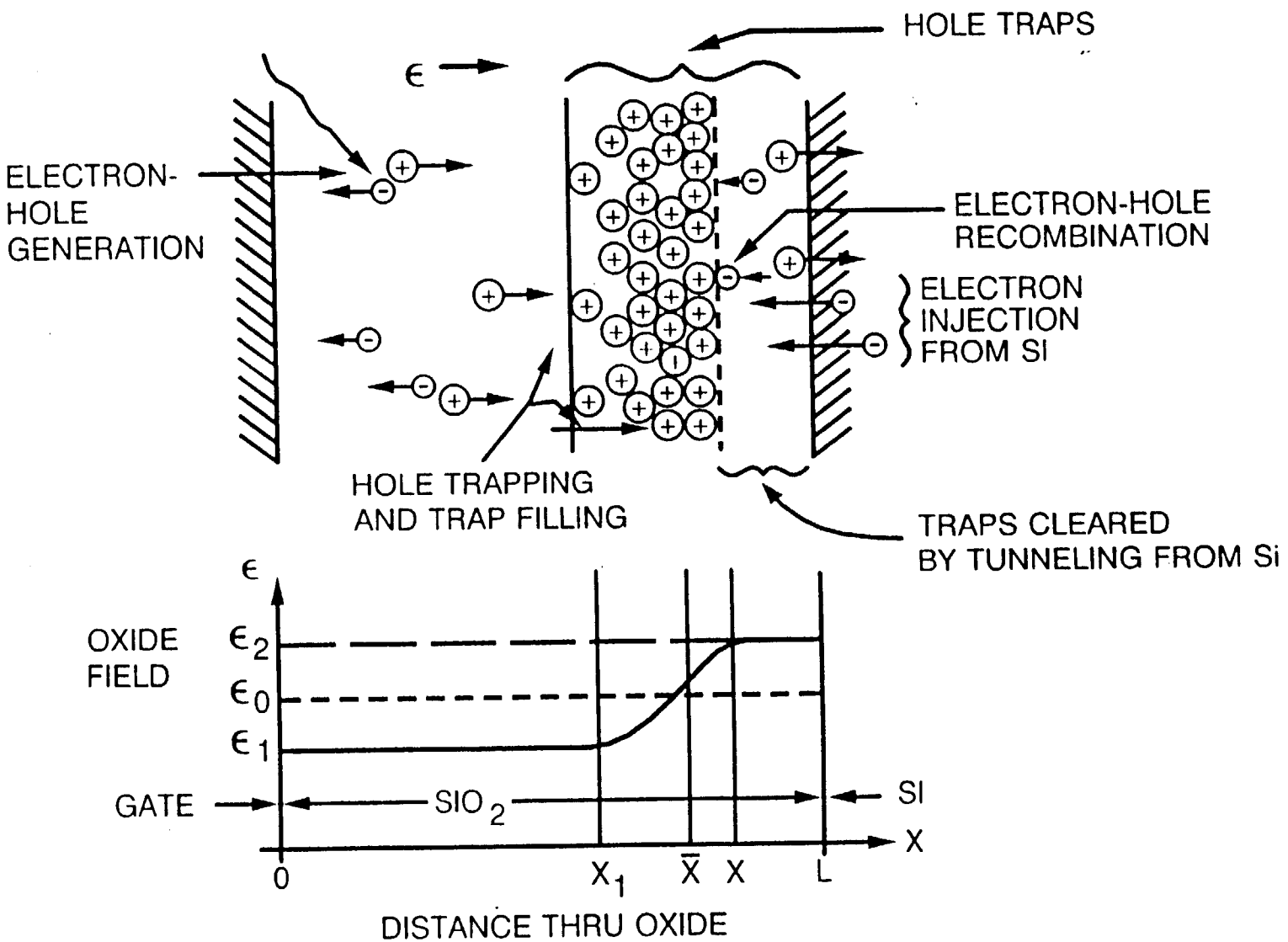

Fig. 12. Charge buildup and removal processes in MOS structure. (A) Schematic of processes. (B) Electric field in oxide layer.

D25.009

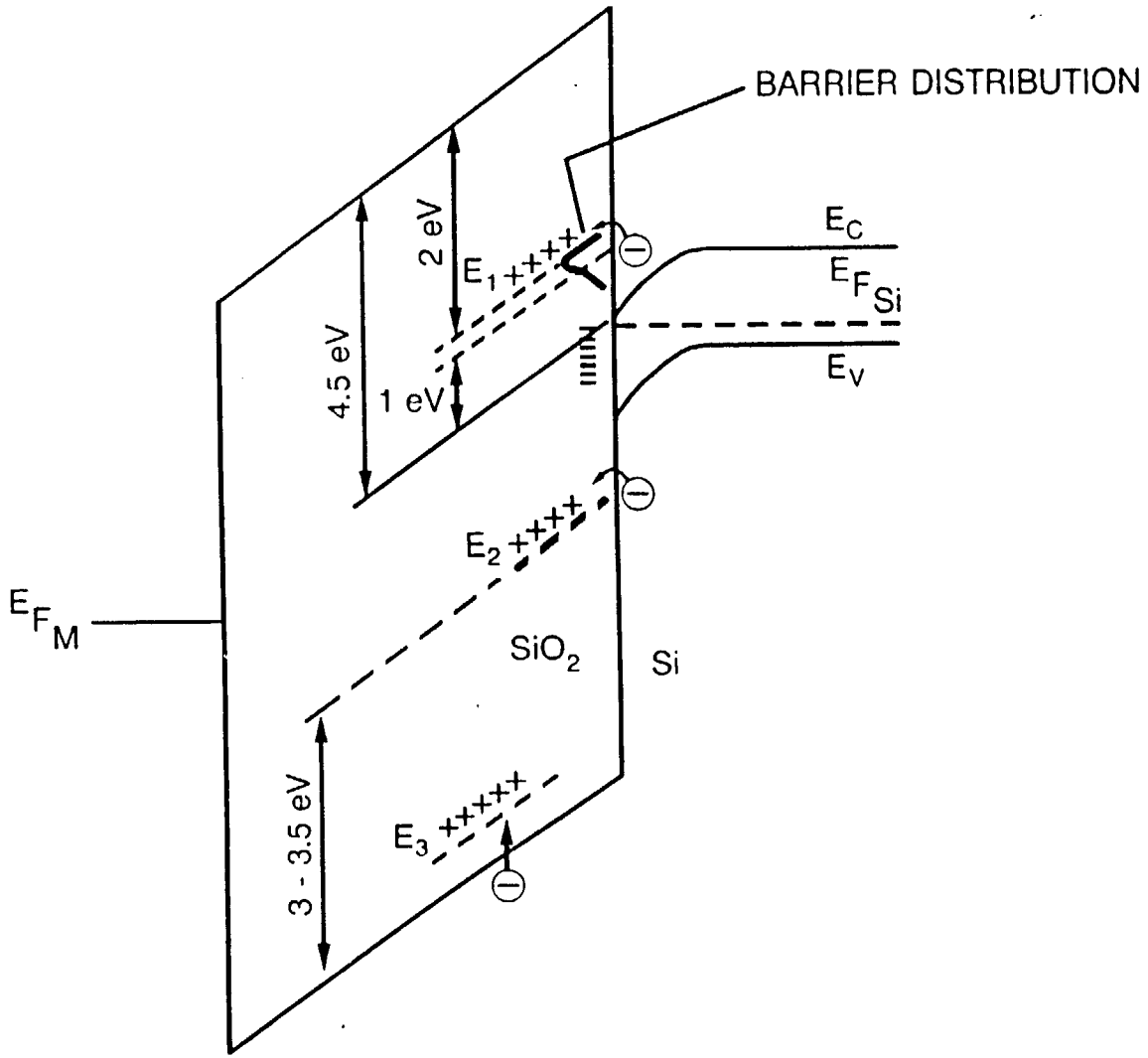

Fig. 13. Energy band diagram of MOS transistor with positive gate bias. Three possible oxide trap locations E_1, E_2, E_3 are shown.

D25.010

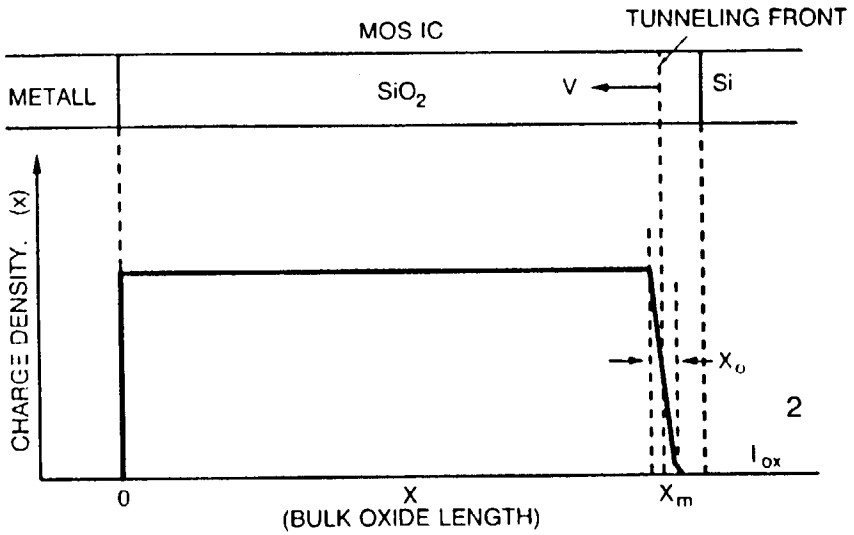

FIG. 14. The charge distribution inside the bulk oxide of MOS device at a time when annealing occurs

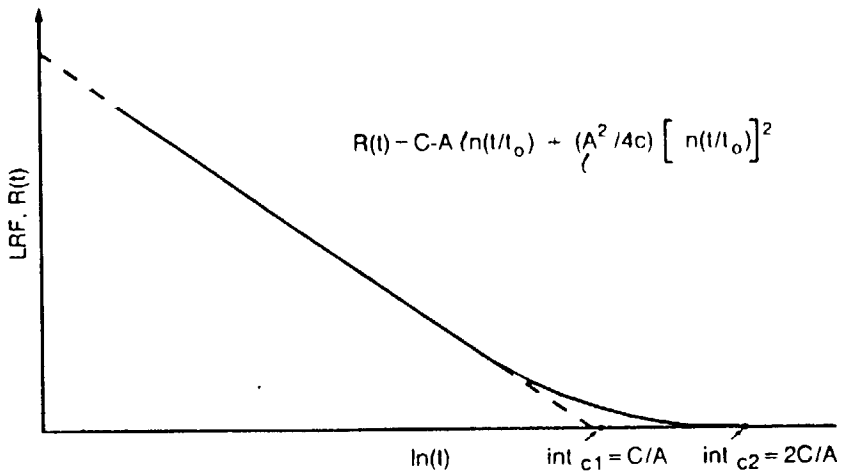

Fig. 15. Linear Response function with non-linear term vs. log(t)

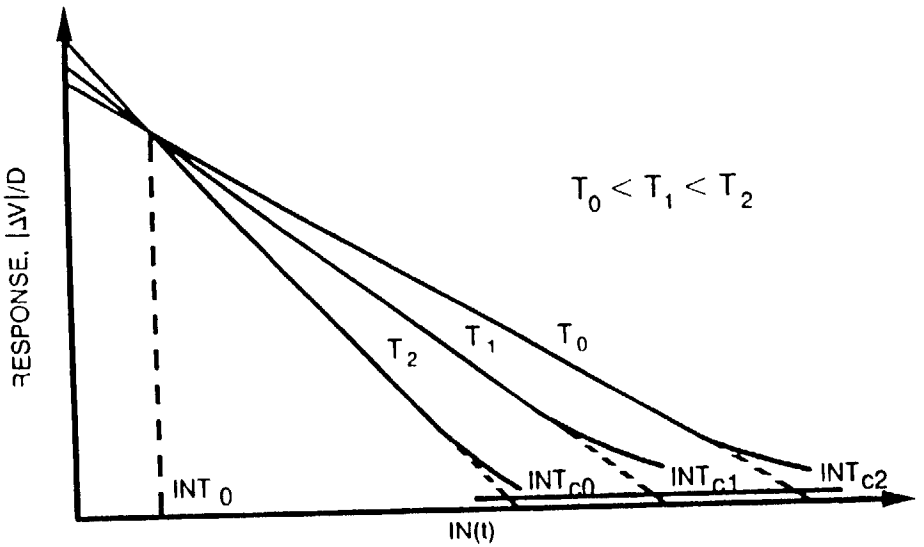

Fig. 16. Family of curves of $\Delta V(t)$ per unit dose at various temperatures.

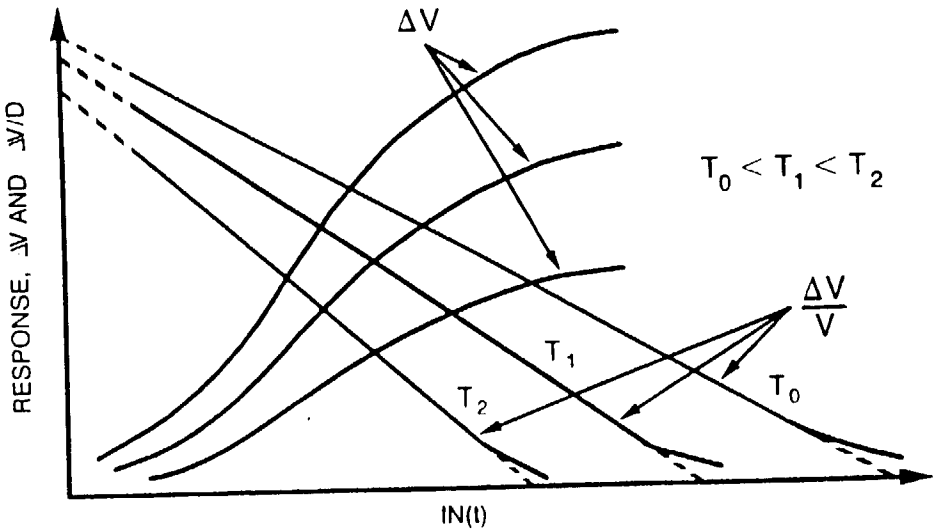

Fig. 17. Family of $\Delta V(t)$ and $\Delta V(t)/D(t)$ curves at various temperatures.

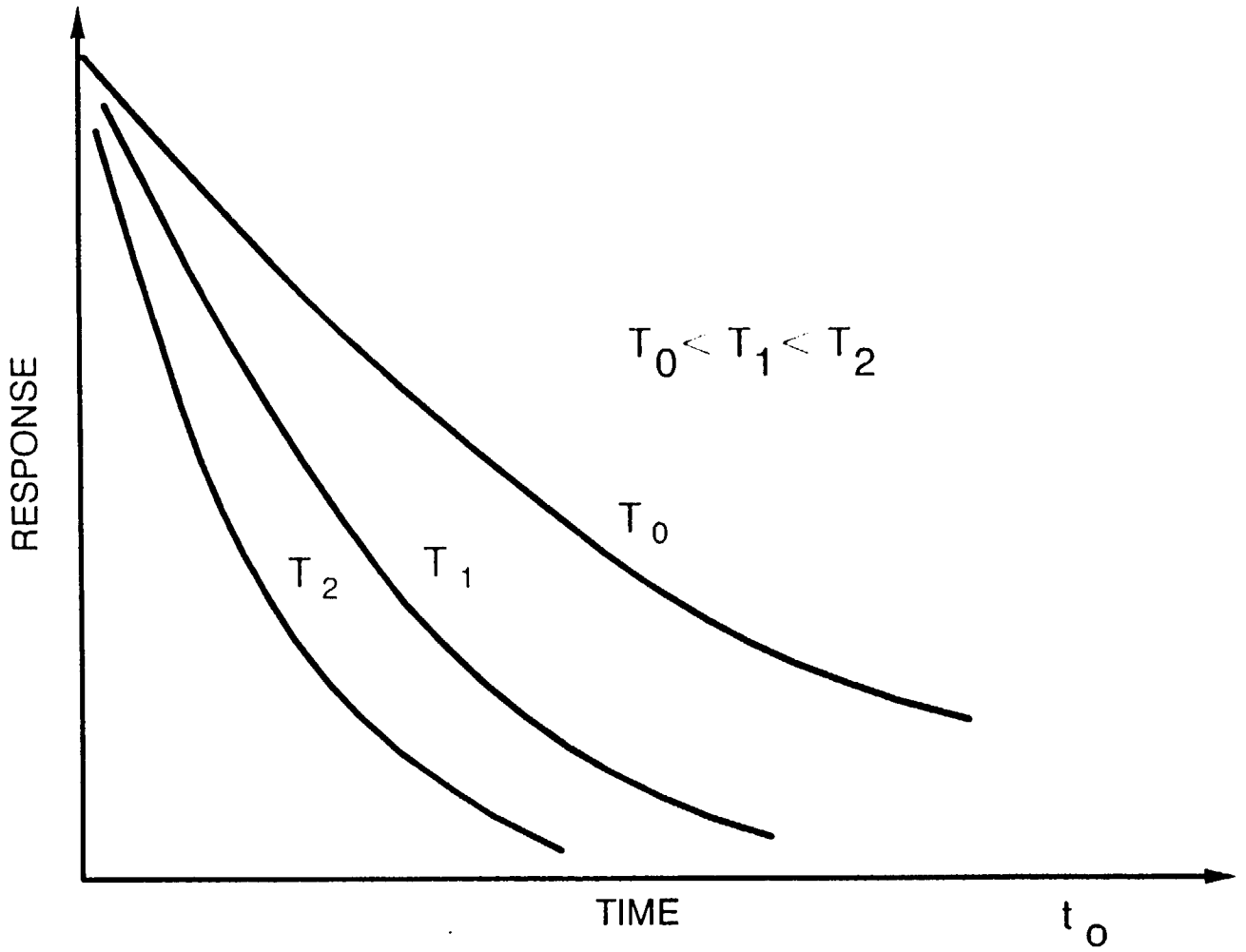

Fig. 18. Pure annealing response function $[\Delta V(t)]$ vs. t for $t<t_o$.

D25.013

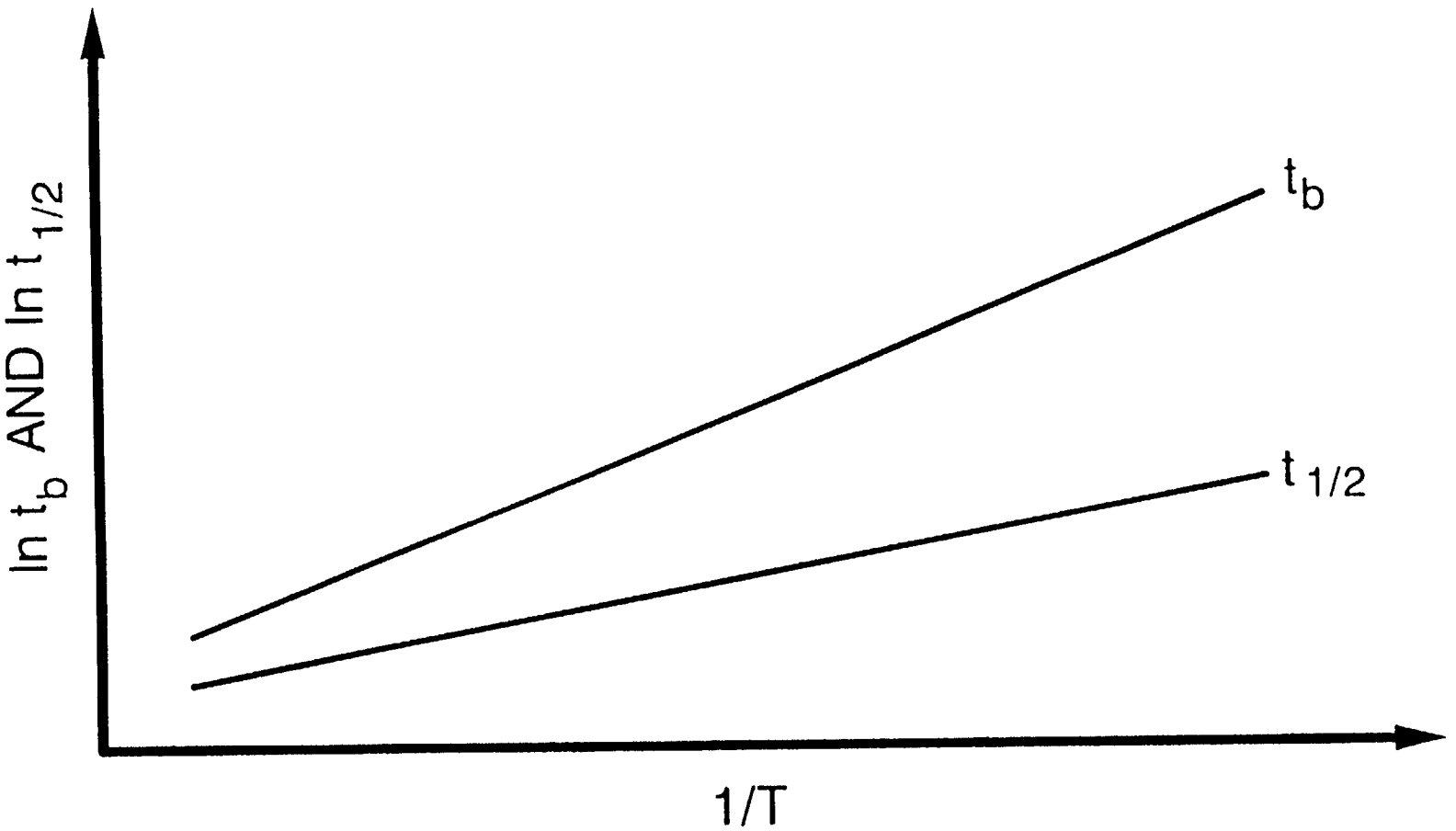

Fig. 19. Temperature dependence of equilibrium (balance) time, t_b, and time for half recovery, $t_{1/2}$

D25.014

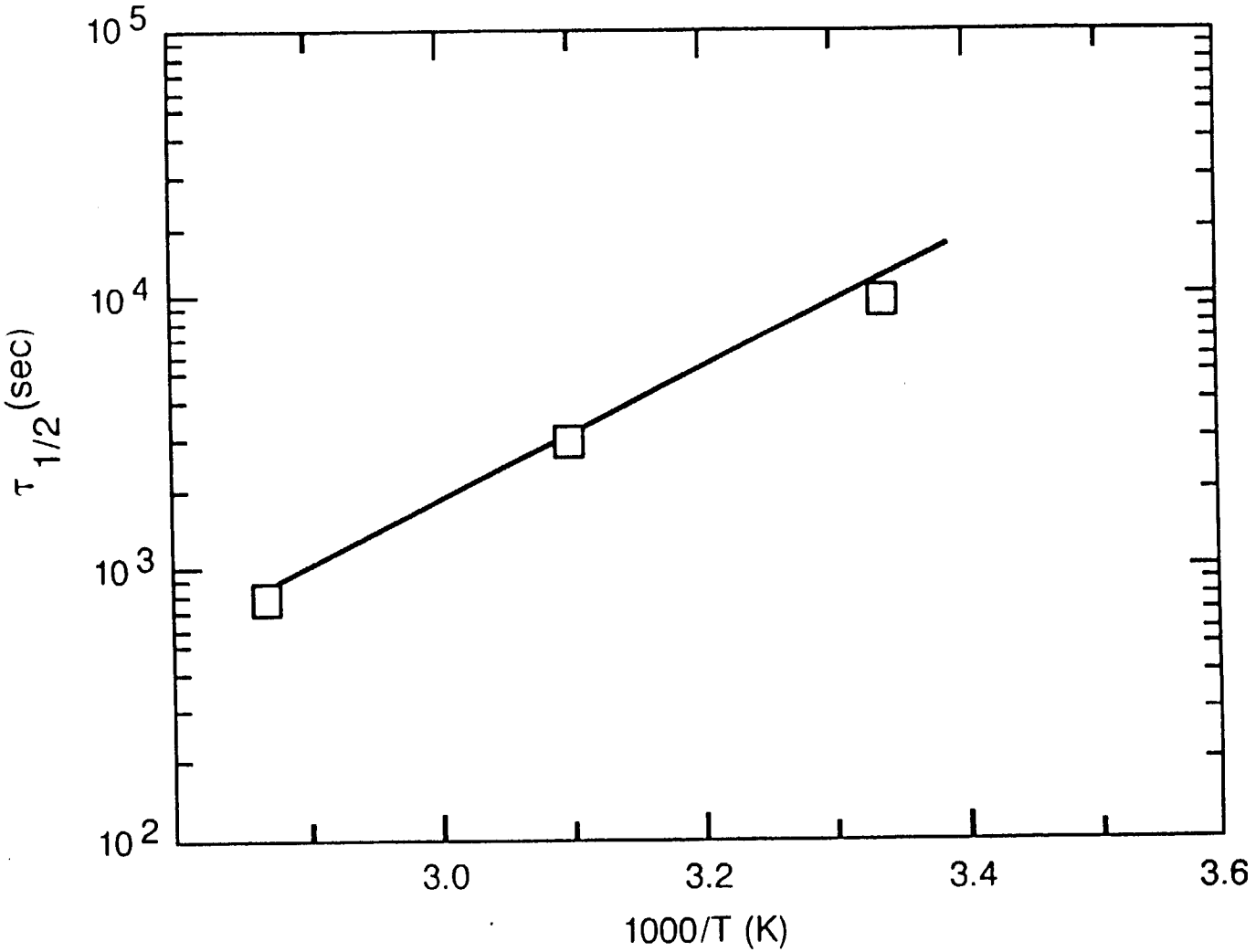

Fig. 20. Time for half recovery of ΔV is plotted against reciprocal of temperature.

D25.015

$$R(t) = R_1(t) + R_2(t) + \ldots + R_n(t)$$

$$R_1(t) = -C_1 + \left[A_1 \ln(t)\right] / \left[1 + \left\{(t/\exp(C_1/A_1)\right\}^2\right]$$

$$R_2(t) = -C_2 + \left[A_2 \ln(t)\right] / \left[1 + \left\{(t/\exp(C_2/A_2)\right\}^2\right]$$

$$\vdots$$

$$R_n(t) = -C_n + A_n \ln(t)$$

IN THIS EXPERIMENTAL CASE:

$R(t) = R_1(t) + R_2(t)$, WHERE:

$$R_1(t) = -C_1 + \left[A_1 \ln(t)\right] / \left[1 + \left\{(t/\exp(C_1/A_1)\right\}^2\right]$$

$$R_2(t) = -C_2 + A_2 \ln(t)$$

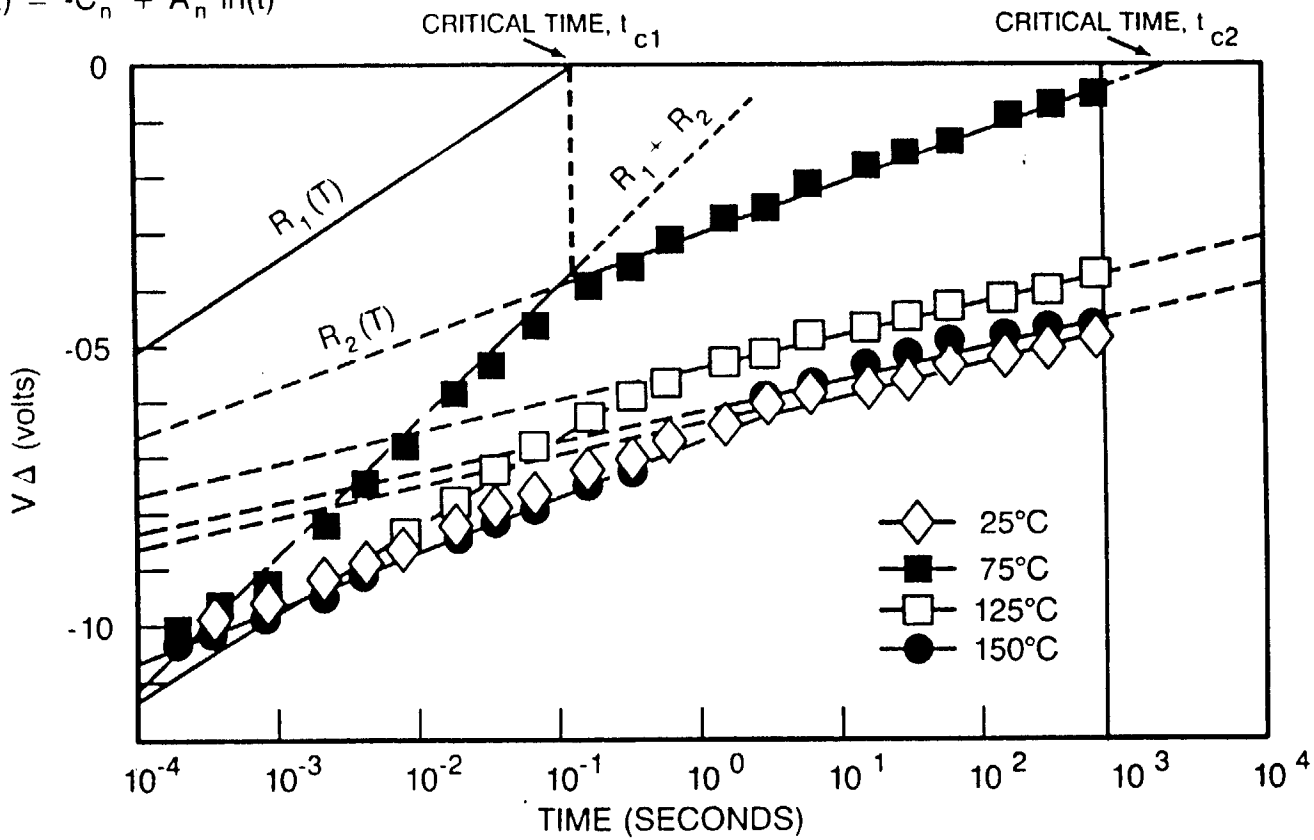

FIG. 21 Application of Linear Response Theory to experimental data at elevated temperatures

D25.016

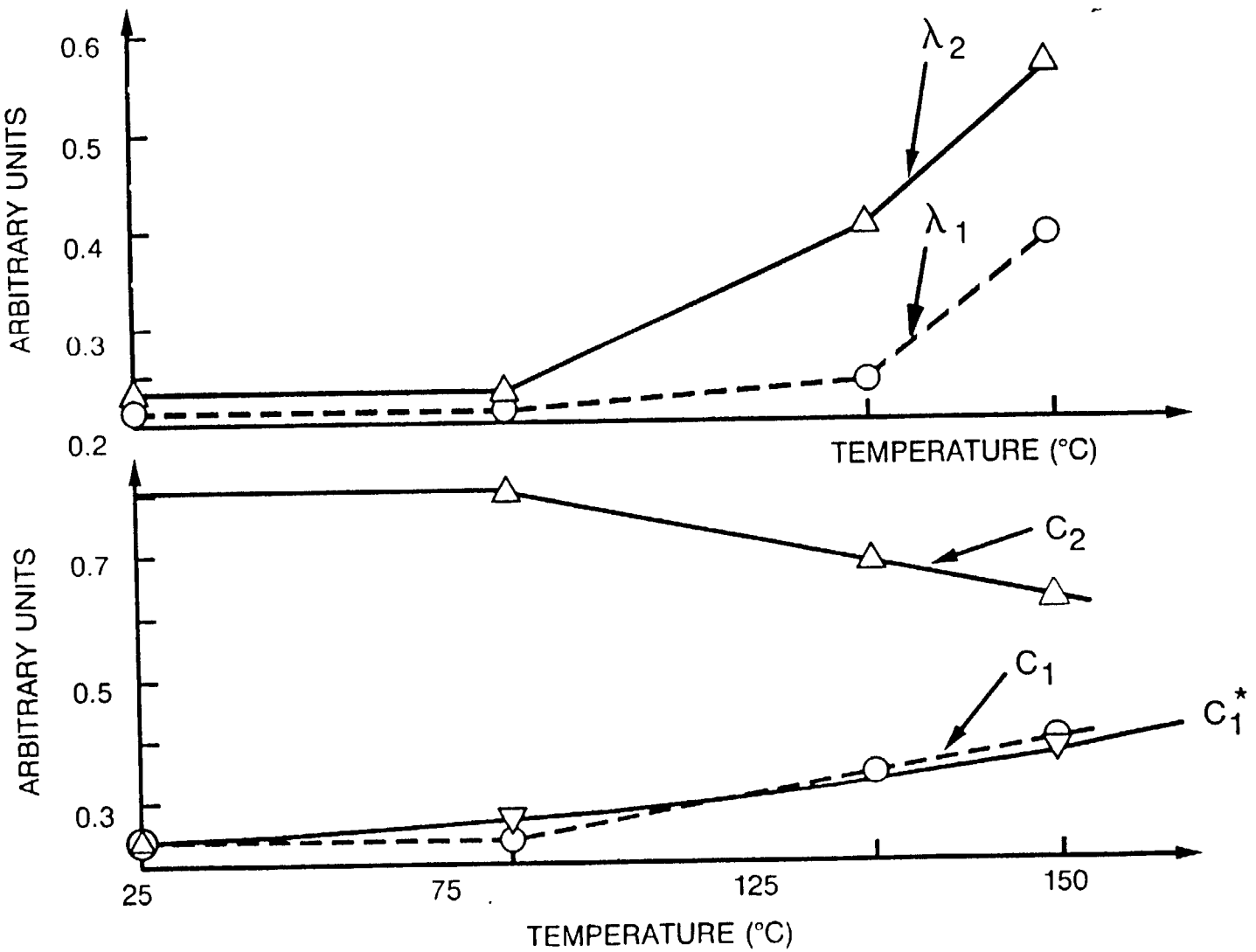

Fig 22. Constants of Linear Response Function for experimental data plotted against temperature. Constant, C_1^*, is calculated from the thermal model.

D25.017

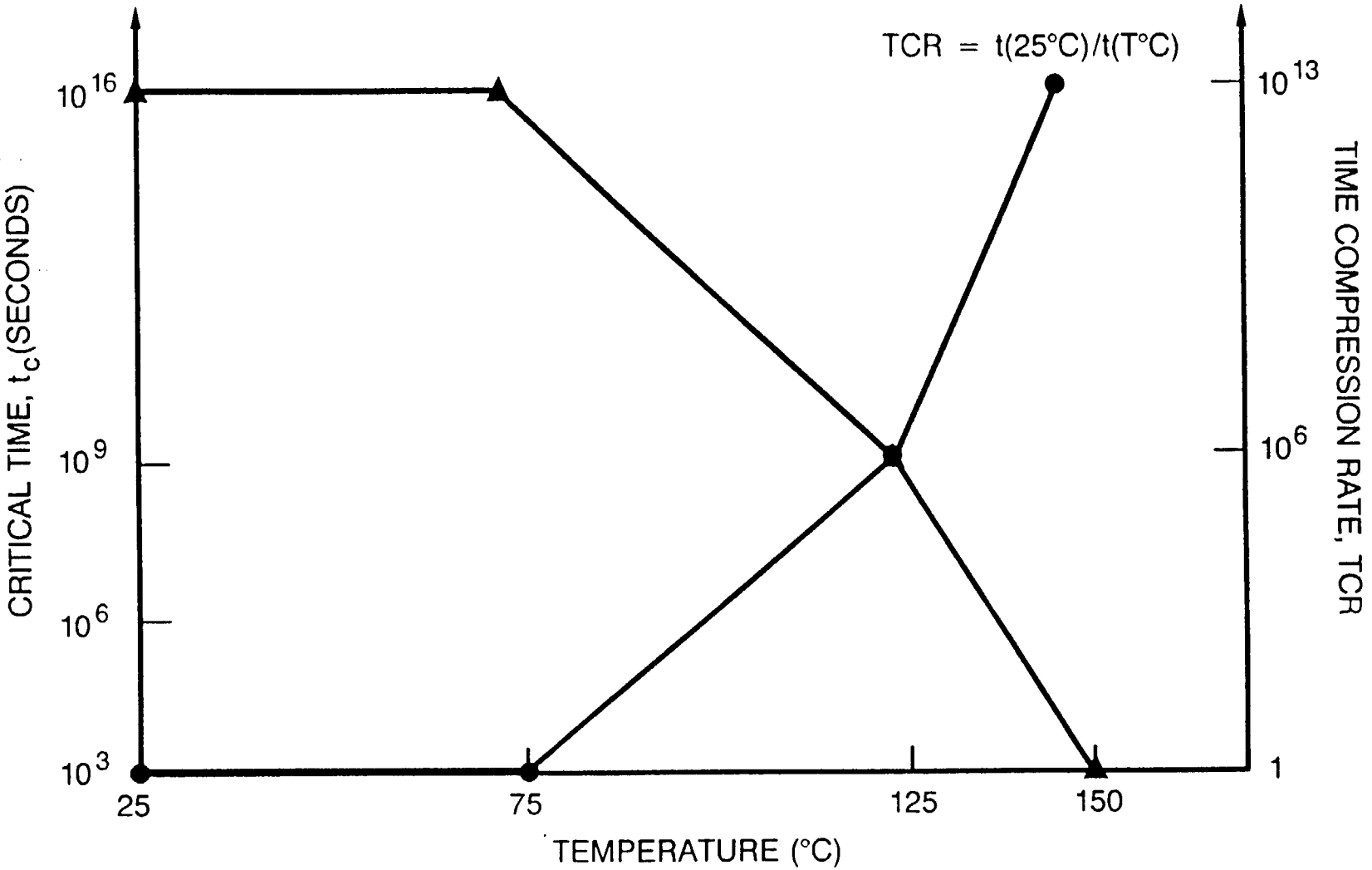

Fig. 23. Time compression rate (TCR) of annealing and critical time versus temperature

D25.018

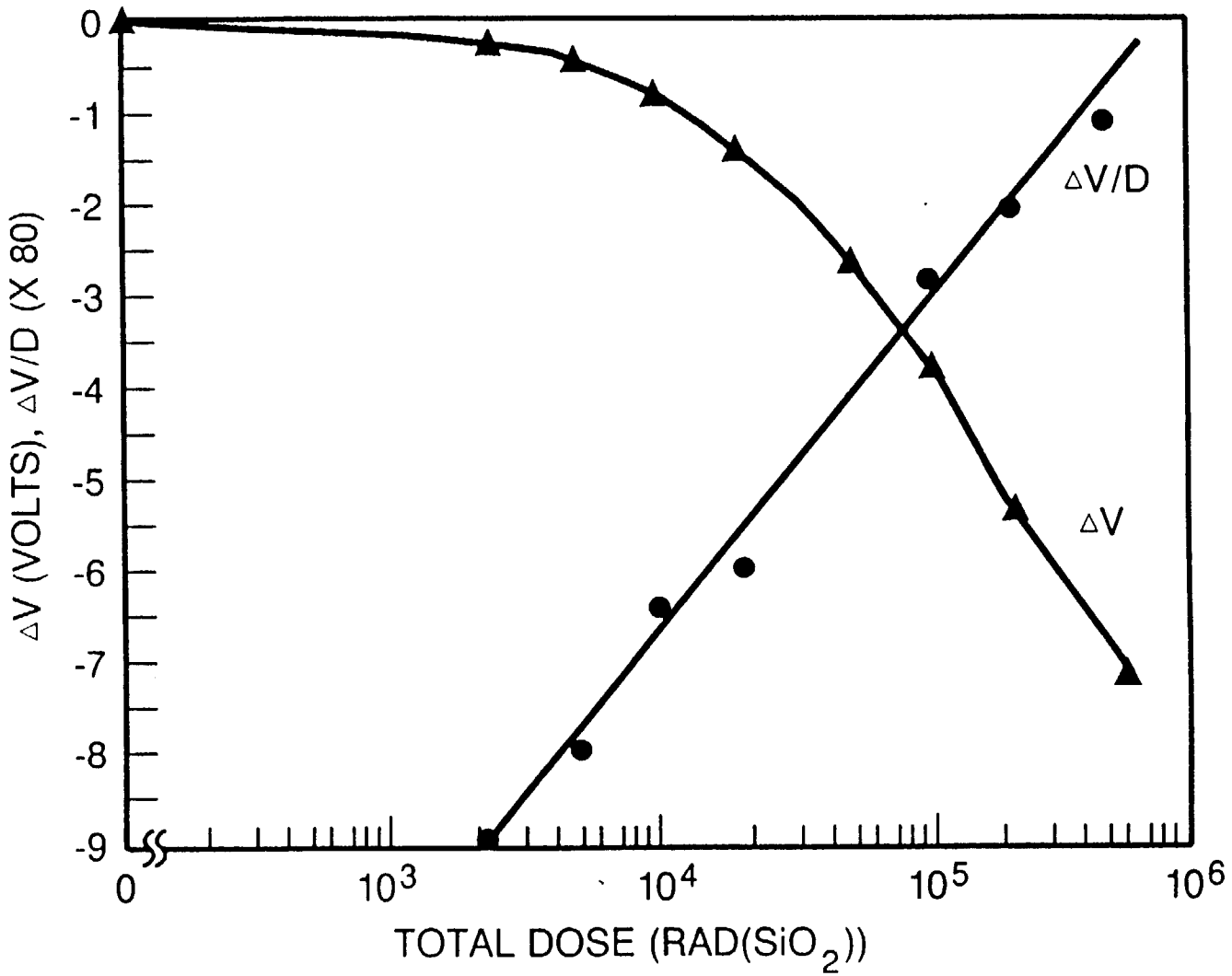

Fig. 24. Voltage shift due to trapped holes versus total dose and voltage shift (mulitple by 80) divided per total dose versus total dose

D25.019

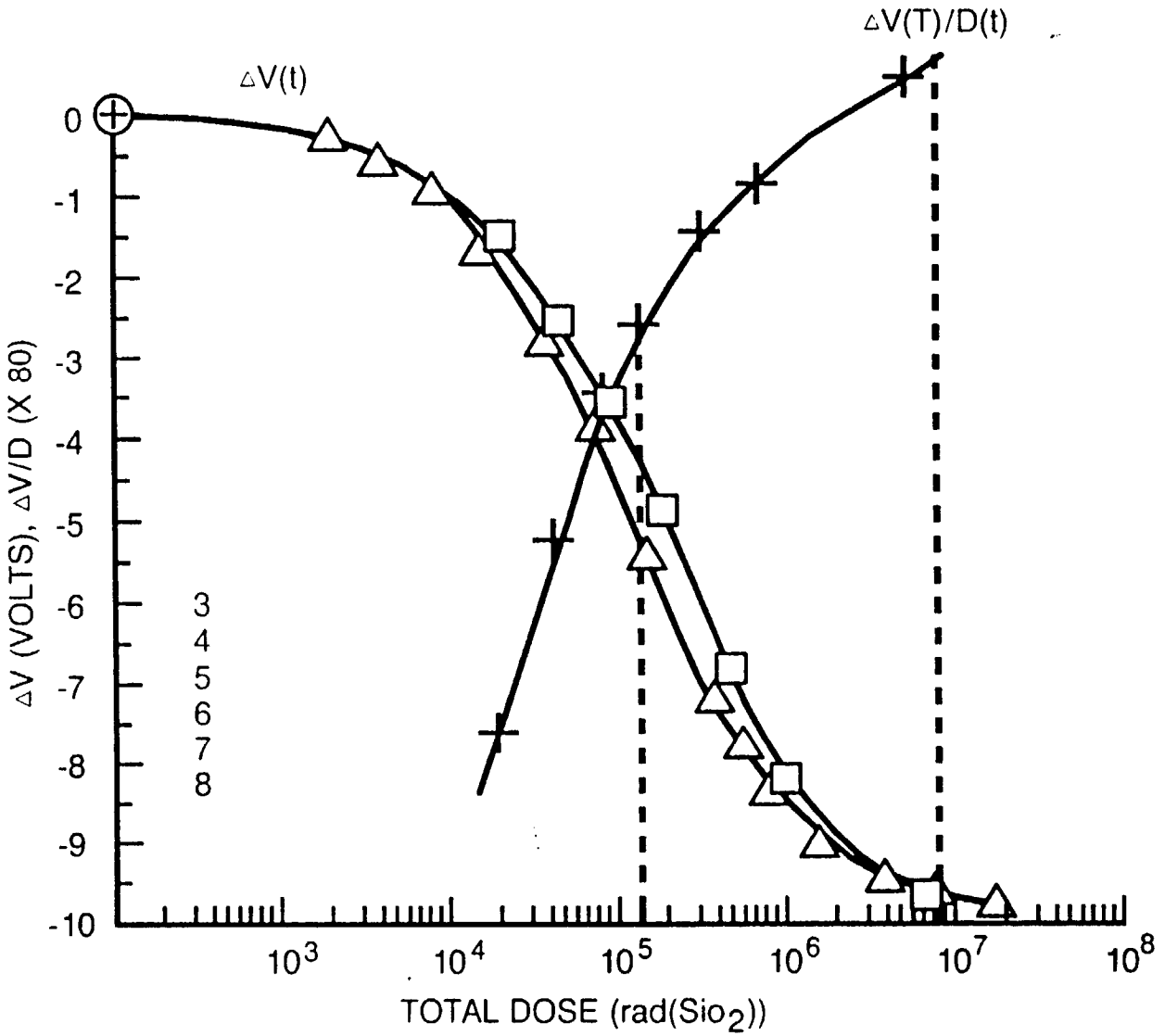

Fig. 25. Voltage shift due to trapped holes versus total dose and voltage shift (multiply by 80) divided per total dose versus total dose.

D25.020

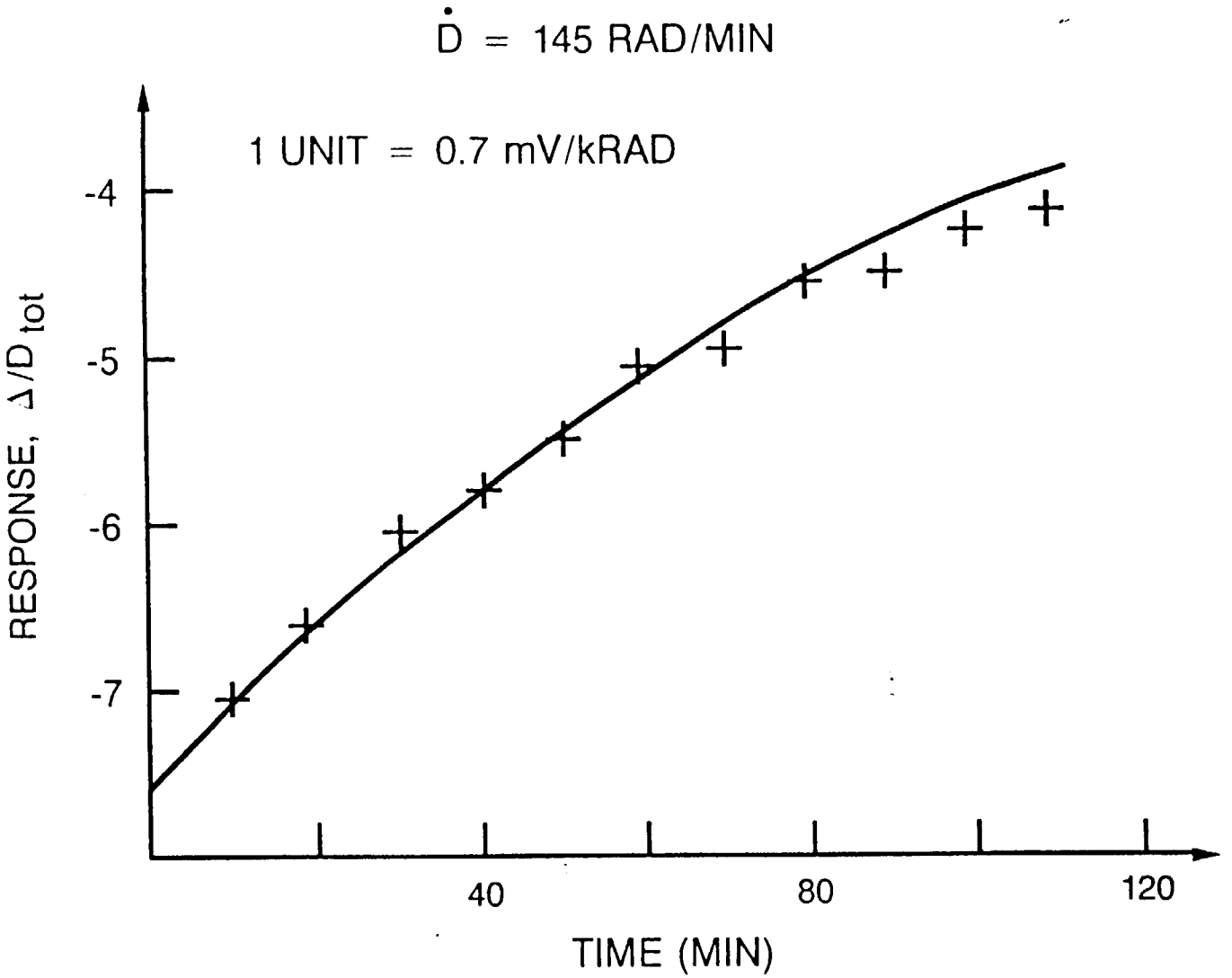

Fig. 26. $\Delta V/D$ for p-channel MOS transistor

D25.021

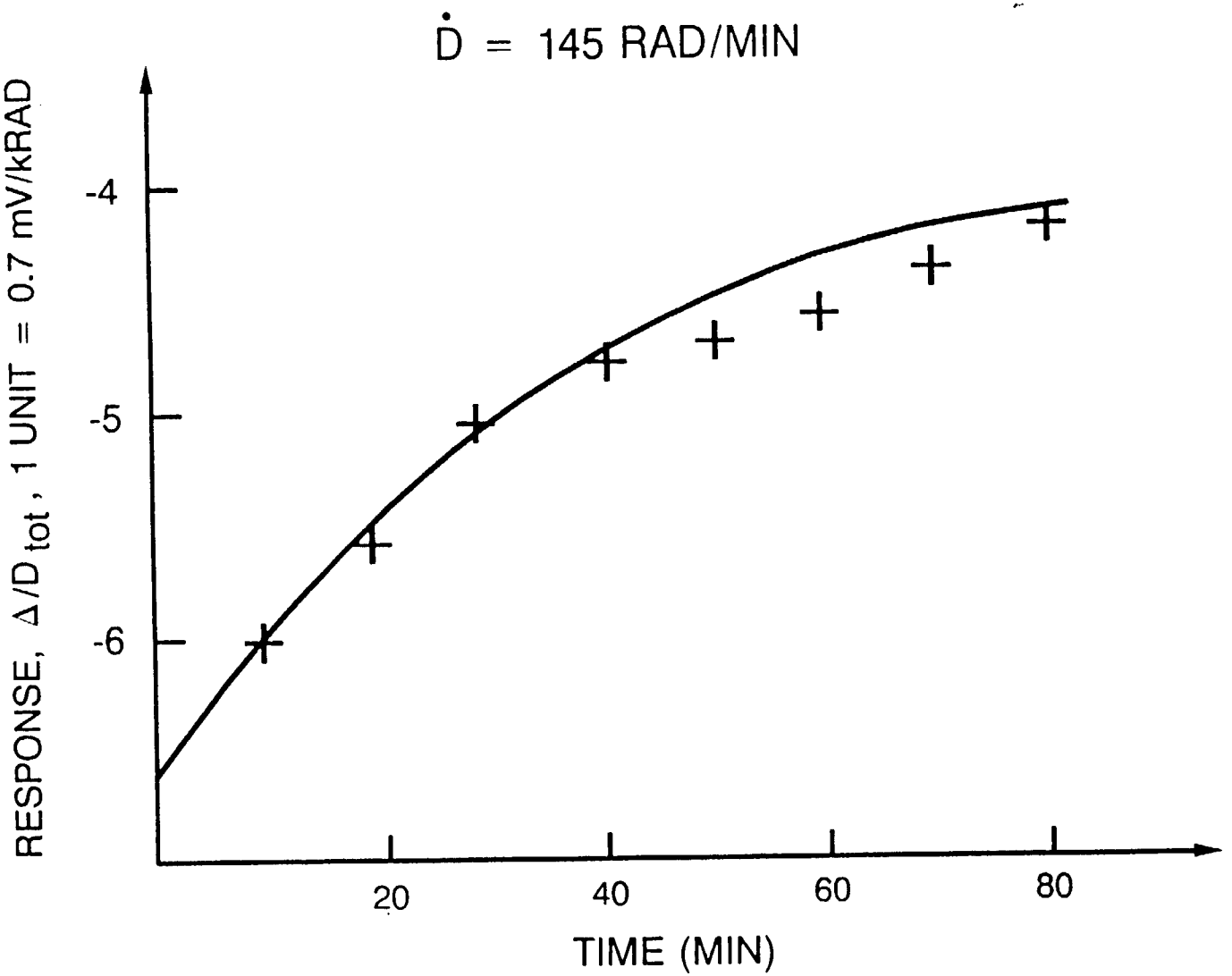

Fig. 27. $\Delta V/D$ for n-channel MOS transistor

D25.022